Bull Volcanol (2006) 68: 516–537
DOI 10.1007/s00445-005-0027-4

RESEARCH ARTICLE

Yasuhiro Ishimine

Sensitivity of the dynamics of volcanic eruption columns to their shape

Received: 16 December 2004 / Accepted: 29 August 2005 / Published online: 10 January 2006
© Springer-Verlag 2005

Abstract This paper presents a one-dimensional steady-state model to investigate the sensitivity of the dynamics of sustained eruption columns to radius variations with height due to thermal expansion of the entrained air, and decreases in atmospheric pressure with height. In contrast to a number of previous models using an equation known as the entrainment assumption, the new model is based on similarity arguments to derive an equation set equivalent to the model proposed by Woods [Bull Volcanol 50:169–193, 1988]. This approach allows investigation of the effect of gas compressibility on the entrainment rate of ambient air, which has been little examined for a system in which a decrease in pressure significantly affects the density stratification of a compressible fluid. The new model provides results that include two end members: one in which the volume change within the eruption columns affects only the radial expansion without changing the vertical motion, and the other is the converse. The Woods [Bull Volcanol 50:169–193, 1988] model can be regarded as being between those two end members. The range of uncertainty arises because the extremely high temperature of discharged materials from a volcanic vent, and the exceptional terminal height of the eruption columns, allow significant expansion of the gas component in the eruption columns, making them behave differently from common turbulent plumes. This study indicates that the maximum height of the eruption columns is affected considerably by this uncertainty, particularly when the eruption columns extend above a height of 10 km, at which the pressure is about one-fourth the pressure at the ground surface. Column collapse may also be suppressed in wider parameter ranges than previously estimated. However, the uncertainty can be reduced by measuring column radii through a vertical profile during actual volcanic eruptions. Accordingly, this paper suggests that appropriate observation of eruption column shapes is essential for improving our understanding of the dynamics of eruption columns.

Keywords Eruption column · Compressibility · Entrainment assumption · Similarity argument

Editorial responsibility: J.D.L. White

Y. Ishimine (✉)
National Research Institute for Earth Science and Disaster Prevention,
3-1 Tennodai, Tsukuba, Ibaraki 305-0006, Japan
e-mail: ishimine@bosai.go.jp
Tel.: +81-29-863-7521
Fax: +81-29-851-5658

Introduction

Volcanic eruption columns are generated during explosive volcanic eruptions that tear magma into fragments and discharge them as pyroclasts from a volcanic vent at speeds of hundreds of meters per second. An eruption column predominantly consists of a turbulent suspension of hot pyroclasts, volcanic gases, and air mixed from the surroundings. Some eruption columns extend as high as 50 km into the atmosphere and sustain themselves for a few hours to several days with a magma discharge rate of 10^6 to 10^9 kg s^{-1} (Walker 1981; Carey and Sigurdsson 1989).

Extensive studies over the last few decades have led to considerable advances in understanding the dynamics of volcanic eruption columns, as summarized in some outstanding reviews (e.g. Woods 1993; Sparks et al. 1997; Dobran 2001). These studies suggest that the lower part of an eruption column is denser than the ambient air and driven by the upward momentum from a volcanic vent. This part is referred to as the gas-thrust region. The eruption column collapses to the ground surface to form a fountain that feeds a pyroclastic gravity current if the column remains denser than the ambient air. However, many eruption columns continue rising because hot pyroclasts contain substantial thermal energy, by which the air mixed into the eruption column is heated and expands to become buoyant. Buoyancy forces generated by thermal energy released from hot pyroclasts dominate the motion at the upper part of the eruption column, which part is referred to as the convective region. The top of an eruption column is called

the umbrella region, at which the eruption column spreads laterally when the bulk density of the gas-particle mixture in the eruption column becomes equal to the density of the ambient atmosphere at that height.

Previous theoretical studies on the dynamics of volcanic eruption columns have been based primarily on classical one-dimensional steady-state models of turbulent jets and plumes. Wilson (1976) investigated the motion of the gas-thrust region by adapting the jet theory of Prandtl (1952). Settle (1978) and Wilson et al. (1978) considered that buoyancy forces dominate the motion of an eruption column at most of its height, and applied the one-dimensional model for turbulent plumes proposed by Morton et al. (1956). They successfully demonstrated that the maximum height of an eruption column has a simple relationship with the heat flux given at a volcanic vent. Woods (1988) combined the jet model of Prandtl (1952) and the plume model of Morton et al. (1956) to develop a more sophisticated one-dimensional steady-state model, which takes the conservation of thermal energy into account to investigate the influences of considerable changes in the density and temperature in an eruption column.

While Woods (1988) successfully shed new light on the dynamics of volcanic eruption columns, the Woods (1988) model involves some conceptual simplifications with relatively few physical variables. In particular, the entrainment assumption, which was introduced by Morton et al. (1956) to parameterize mixing between the inside and outside of turbulent plumes, plays a key role in the Woods (1988) model. The entrainment assumption has been justified by laboratory experiments under simple conditions and applied to phenomena over a wide range of scales (Turner 1986). However, physical observations during actual volcanic eruptions are too sparse to ensure that the entrainment assumption can be applied to eruption columns.

Volcanic eruption columns involve a number of physical processes that are not considered in the original plume model of Morton et al. (1956). The physical processes that cause volume changes to a gas-particle mixture in an eruption column may violate the entrainment assumption because the entrainment assumption is originally introduced to an incompressible fluid flow. Therefore, the influence of the thermal expansion of mixed air due to heat exchange between hot particles and the surrounding gas should be carefully examined. A decrease in atmospheric pressure with height also needs to be addressed because it causes considerable expansion of an uprising gas-particle mixture in an eruption column that is as high as the scale height of the atmosphere.

A possible approach to investigate the effects is to conduct computer simulations. Elaborate numerical models based on the Navier-Stokes equations have been developed in the past two decades to provide abundant information on eruption columns (e.g. Valentine and Wohletz 1989; Neri and Dobran 1994; Oberhuber et al. 1998). Computer simulations will be an increasingly influential approach because they have a significant potential for investigating realistic complex processes, including time-variable and three-dimensional effects.

Despite that, special care is required to evaluate simulation results, particularly those related to the processes addressed here, primarily because numerical techniques for compressible flows of a gas-particle mixture are still in their infancy. The thermal expansion of a gas-particle mixture is controlled by the intimate interaction of the thermal and particle diffusion due to turbulence, whose length scale is substantially smaller than a typical grid size of volcanic simulations. The validity of numerical methods for approximating the contribution of the process is scarcely ascertained. Expansions due to pressure changes also tend to induce considerable errors in computer simulations because inappropriate conditions such as unrealistic boundaries often smear pressure calculations. Therefore, the quantitative accuracy of simulation results is open to question.

Simulation results should be interpreted on the basis of the proper understandings of the significance of particular effects on flow characteristics, many of which are gained from similarity arguments. This suggests that similarity arguments are still useful even in the computer age. This study aims to provide a physical basis for robust simulations with a well-designed numerical model. The outcome of this study is used to extend the numerical model presented in Ishimine (2005) to appropriately calculate eruption columns penetrating the stratosphere.

This paper discusses how the thermal expansion of mixed air and the decrease in atmospheric pressure affect the formulation of the simple one-dimensional model based on similarity arguments. The focus is primarily on the modification required of the entrainment assumption, which is used in the same form as in Morton et al. (1956) in previous studies that examine gas compressibility in eruption columns (e.g., Sparks 1986; Woods 1988; Glaze and Baloga 1996).

This paper does not address some effects that play important roles in the dynamics of eruption columns, for example, thermal disequilibrium between particles and the surrounding gas, excessive pressure of ejected materials, and condensation/evaporation of magmatic and atmospheric water. The additional processes are ignored to prevent obscuring the central point of this paper. I adopt the simple assumptions used in Woods (1988) except for the entrainment assumption. This approach leads to development of a new model of sustained eruption columns analogous to the Woods (1988) model. The comparison of the models provides insight into the dynamics of eruption columns. The additional processes are expected to affect the new model in a similar manner as the previous models. They are easily incorporated into the new model because the mathematical formulations for the processes have been proposed in previous studies (e.g., Woods and Bursik 1991; Woods and Bower 1995; Glaze et al. 1997).

The first part of this paper is devoted to reviewing one-dimensional steady-state models of turbulent jets and plumes with the help of similarity arguments. This may clarify the physical background of the entrainment assumption for turbulent jets and plumes in uniform surroundings. The mathematical treatment for deriving one-dimensional

steady-state models that include the effect of the thermal expansion of mixed air and the decrease in atmospheric pressure is then examined. An alternative formulation of an eruption column is proposed on the basis of the above discussion, to examine the sensitivity of the vertical variation of physical variables, such as the density, temperature, and upward velocity in an eruption column, on the variation in radius with height. There are five appendices, which contain derivations of various equations to support the arguments in the main body of the paper.

Similarity solutions of turbulent jets and plumes

Fundamental assumptions

As in previous studies of volcanic eruption columns, I assume eruption columns to be generated by continuous discharge of a hot mixture of magma fragments and volcanic gases from a volcanic vent. I use a one-dimensional steady-state model for a forced plume. A forced plume is a flow caused by continuous discharge of a fluid from a small orifice into another fluid, which is at rest when not influenced by the discharged fluid. The vigorous turbulent mixing between the discharged fluid and the ambient fluid gives the forced plume a characteristic conical shape.

The flow is referred to as a turbulent jet if the density of the discharged fluid is virtually equal to the density of the ambient fluid and, as a result, the buoyancy effect is negligible. A turbulent jet is driven by the momentum flux given at the orifice. If the density difference between the discharged fluid and its surroundings is so significant that the buoyancy effect is predominant over the effect of the momentum flux from the orifice, then the flow is referred to as a turbulent plume, or a pure plume, to distinguish it from a forced plume. A forced plume is affected by buoyancy forces as well as the momentum flux from the orifice. A forced plume is sometimes referred to as a buoyant jet.

I first review one-dimensional steady-state models of turbulent jets and turbulent plumes to provide a theoretical framework to discuss eruption columns. These flows have been widely studied as a basic problem of fluid dynamics and the results may be found in the literature (e.g. Fischer et al. 1979; List 1982; Turner 1986).

Similarity solutions for the time-averaged properties of idealized turbulent jets and plumes can be obtained under the assumptions listed below. Note that numbers (1) through (8) are considered wholly acceptable for the purpose of this paper even when applying to eruption columns, while numbers (9) and (10) are subsequently addressed in more detail.

(1) Flows are so extremely turbulent that viscosity does not affect the flow.
(2) Flows can be regarded as steady when considering temporal averages over an appropriate period of time, despite flows being turbulent and thus inherently unsteady.
(3) Flows of the surrounding fluid are negligible except for the turbulent region affected by the discharged fluid.
(4) The difference in pressure between inside and outside of the turbulent region is negligible.
(5) Boundaries do not affect the flows.
(6) Buoyancy forces and the momentum supplied from a source are both directed vertically upward. Accordingly, horizontal motion is negligible.
(7) The time-averaged profiles of vertical velocity and density in a horizontal cross-section are similar at all heights.
(8) An orifice is infinitely small and thus the shape and size of the orifice do not affect flows.
(9) Both the discharged and surrounding fluids are incompressible and do not change volume upon mixing.
(10) The density difference between the discharged and surrounding fluids is small compared with the reference density, which in this paper is the density of the surrounding fluid at the level of the source.

Physical variables are described in cylindrical polar coordinates (r, z), where the vertical axis is taken as the z-axis with its origin at the injecting source, and the perpendicular distance from the z-axis is denoted by r. My interest in this section is in determining the variation of the time-averaged profile of the upward velocity, $w'(r, z)$, and density, $\rho'(r, z)$, with height. Previous experimental studies of jets and plumes suggested that time-averaged profiles in the horizontal cross-section are axially symmetrical and described well by Gaussian profiles, as

$$w'(r, z) = w(z) \exp\left(-\frac{r^2}{L^2}\right), \tag{1}$$

and

$$\rho'(r, z) = \alpha(z) - \Delta\rho(z) \exp\left(-\frac{r^2}{\lambda^2 L^2}\right), \tag{2}$$

where $w(z)$ is the upward velocity on the z-axis, $\alpha(z)$ is the density of the ambient fluid, $\Delta\rho\ (z)$ is the difference of the density on the z-axis from the ambient density, L is the horizontal length scale on which the upward velocity decays by a factor $1/e$, and λ is the ratio of the length scale of the density distribution to that of the upward velocity distribution (all variables used in this paper are listed in Table 1).

Laboratory experiments indicate that λ tends to be slightly greater than unity. For example, Rouse et al. (1952) give λ=1.16 for forced plumes generated by heated air, while Papanicolaou and List (1988) report that λ=1.194 for forced plumes of sodium chloride-water solutions. In this paper, I define the length scale L as the radius of the flow for simplicity, on the assumption that λ is unity.

The motion of turbulent jets and plumes is described by the conservation conditions of volume, mass, and momentum; therefore, I discuss the three vertical fluxes integrated across the horizontal cross-section at each height.

Table 1 Notations

B	Buoyancy flux
B^*	Buoyancy flux modified by pressure decrease
B_o	Buoyancy flux at the source
C	Integration constant
C_a	Specific heat at a constant pressure of the air, 998 J K^{-1} kg^{-1}
C_P	Bulk specific heat at a constant pressure of the material in the eruption column
C_{Po}	Bulk specific heat at a constant pressure of the material in the eruption column at the source, 1617 J K^{-1} kg^{-1}
g	Gravitational acceleration, 9.81 m s^{-2}
H_1	Height of the tropopause, 11 km
H_2	Height of the stratopause, 20 km
h_a	Characteristic length scale for an isentropic atmosphere
h_j	Characteristic length scale for a forced plume
k_j	Jet radius gradient, 0.125
k_p	Plume radius gradient, 0.108
L	Radius
L^*	Radius modified by pressure decrease
$L^\dagger$	Modified radius for the eruption column
L_o	Radius at the source
M	Momentum flux
M_o	Momentum flux at the source
m_g	Mass of gas in the eruption column at a given height
m_m	Mass of volcanic gas in the eruption column at a given height
m_s	Mass of solid particles in the eruption column at a given height
N	Brunt-Väisälä frequency
n	Gas mass fraction
n_o	Gas mass fraction at the source
P	Pressure
P_o	Pressure at the ground surface
P_1	Pressure at the tropopause
P_2	Pressure at the stratopause
Q	Mass flux
R	Non-dimensional radius of an incompressible plume in a stratified environment
R^*	Non-dimensional radius of a plume in an isentropic atmosphere
R_a	Gas constant for the air 285 J K^{-1} kg^{-1}
R_g	Bulk gas constant for the gas in the eruption column
R_m	Gas constant for the volcanic gas 462 J K^{-1} kg^{-1}
r	Radial distance from the centerline
T	Temperature in the eruption column
T^*	Temperature of the isentropic air
T_a	Temperature of the ambient air
T_o	Temperature of the ambient air at the ground surface, 273 K
T_1	Temperature of the ambient air at the tropopause
U	Non-dimensional velocity of an incompressible plume in a stratified environment
U^*	Non-dimensional velocity of a plume in an isentropic atmosphere
V	Volume flux
V_e	Volume flux of the entrained fluid per unit height
V_e^*	V_e modified by pressure decrease
$V_e^\dagger$	V_e modified for the eruption column
w	Vertical velocity on the centerline
w'	Local vertical velocity
w_o	Vertical velocity on the centerline at the source
X	$L^* w$
x	Non-dimensional height of an incompressible plume in a stratified environment
x^*	Non-dimensional height of an isentropic atmosphere
Y	$L^{*2} w$
z	Height above the source
α	Density of the environment
α^*	Potential density for α
α_o	Density of the environment at the source height
β	Density on the centerline
β_o	Density on the centerline at the source
Γ_1	Temperature lapse rate at the troposphere, −6.5 K m^{-1}
Γ_2	Temperature lapse rate at the stratosphere, 2.0 K m^{-1}
γ	Ratio of specific heats of the air, 1.40
Δ	Non-dimensional reduced gravity
$\Delta\rho$	Density difference between the centerline and environment, $\alpha-\beta$
$\Delta\rho^*$	$\Delta\rho$ modified by pressure decrease
δV	Volume change of the internal fluid
δV_e	Volume change of the entrained fluid
ε_j	Entrainment coefficient of the jet, 0.0625
ε_p	Entrainment coefficient of the plume, 0.0900
λ	Ratio of the length scale for the velocity and density, 1.0
π	3.14
ρ'	Local density
ρ_b	Density of the air at a temperature in an eruption column
ρ_g	Density of the gas phase in an eruption column
ρ_m	Density of volcanic gas at a temperature in an eruption column
ρ_s	Density of solid particles, 1000 kg m^{-3}
ϕ	Gas volume fraction
ϕ_o	Gas volume fraction at the source
ξ	Non-dimensional variable of X
ψ	Non-dimensional variable of Y

The volume flux $V(z)$ is defined by

$$V(z) = \int_0^\infty w'(r, z) \cdot 2\pi r\, dr. \tag{3}$$

Similarly, the mass flux $Q(z)$ and momentum flux $M(z)$ are defined by

$$Q(z) = \int_0^\infty \rho'(r, z) w'(r, z) \cdot 2\pi r\, dr, \tag{4}$$

$$M(z) = \int_0^\infty \rho'(r, z)\, w'(r, z)\, w'(r, z) \cdot 2\pi r\, dr. \tag{5}$$

Equations (1) and (2) can be used to rewrite Eqs. (3) to (5) as

$$V(z) = \pi L^2 w, \tag{6}$$

$$Q(z) = \pi \left(\alpha - \frac{\lambda^2}{1+\lambda^2} \Delta\rho \right) L^2 w, \tag{7}$$

$$M(z) = \frac{\pi}{2} \left(\alpha - \frac{2\lambda^2}{1+2\lambda^2} \Delta\rho \right) L^2 w^2. \tag{8}$$

Turbulent jets in a uniform environment

A turbulent jet can be defined as a flow generated by continuous discharge of a fluid of a constant density from a small orifice into a calm fluid of the same density. The density difference between the discharged fluid and its surroundings is zero (i.e., $\Delta\rho = 0$), and thus Eq. (8) can be rewritten as

$$M(z) = \frac{\pi}{2} \alpha L^2 w^2. \tag{9}$$

The total momentum flux passing through any horizontal cross-section remains constant when no external forces act on the fluid, i.e.,

$$\frac{\mathrm{d}}{\mathrm{d}z} \left(\frac{\pi}{2} \alpha L^2 w^2 \right) = 0, \tag{10}$$

where $\pi\alpha/2$ can be eliminated because it is constant. Equation (10) indicates that the volume flux described by Eq. (6) approaches zero when L approaches zero. This also holds for the mass flux. Thus, we can envisage a virtual point source from which a finite amount of momentum flux is supplied without volume and mass fluxes. This indicates that the turbulent jet is defined by momentum flux M alone, which remains constant at all distances from the origin.

The above property suggests that an additional constraint can be obtained from similarity arguments, as described in several publications (e.g. Fischer et al. 1979; List 1982; Turner 1986; Landau and Lifshitz 1987). The effect of viscosity is essentially unimportant for the motion considered here because this paper addresses fully turbulent flows to apply to volcanic eruption columns with Reynolds numbers certainly exceeding a few hundred thousands. Turbulent mixing also prevents the shape and size of the orifice from affecting the form of turbulent jets at distances greater than the dimensions of the orifice. Boundary conditions also cannot prescribe the length scale because the solution for flows in a virtually infinite space filled with a calm fluid is now sought. As a result, there are no characteristic parameters with the dimensions of length. The flow properties are thus governed by turbulence alone, which makes the flow self-similar.

If a turbulent jet spreads its radius as geometrically self-similar, the radius can only be directly proportional to the height:

$$L = k_j z, \tag{11}$$

where k_j is a proportionality constant verified by laboratory experiments. The upward velocity can be derived from Eqs. (10) and (11):

$$w = \frac{1}{k_j} \left(\frac{2M}{\pi\alpha} \right)^{1/2} z^{-1}. \tag{12}$$

Although many previous studies on volcanic eruption columns treat the gas-thrust region by adapting Prandtl (1952)'s theory, the above description is preferable because it facilitates comparing the mathematical treatment of turbulent jets with that of turbulent plumes described later. The present treatment is mathematically equivalent to that in Prandtl (1952) for the arguments in this paper. For example, combining Eqs. (10) and (11) with a value obtained from experiments:

$$k_j = \frac{\mathrm{d}L}{\mathrm{d}z} = \frac{1}{8}, \tag{13}$$

yields Wilson (1976)'s Eq. (10):

$$w \frac{\mathrm{d}w}{\mathrm{d}z} = -\frac{w^2}{8L}. \tag{14}$$

Turbulent plumes in a uniform environment

A pure turbulent plume can be defined as a flow driven by buoyancy forces alone. This indicates that the momentum flux given at an orifice is negligible in a pure plume compared with the momentum flux generated by buoyancy forces. The flow properties of a turbulent plume in a uniform environment can thus be determined by simple similarity arguments, as with the turbulent jet described above.

Buoyancy forces act at all heights, and thus the conservation of the momentum flux passing through a horizontal cross-section can be given by

$$\frac{\mathrm{d}M}{\mathrm{d}z} = \int_0^\infty (\alpha - \rho') g \cdot 2\pi r \, dr, \tag{15}$$

where g is the acceleration due to gravity. Integrating the right hand side transforms Eq. (15) to

$$\frac{\mathrm{d}}{\mathrm{d}z} \left(\frac{\pi}{2} \alpha L^2 w^2 \right) = \pi \lambda^2 \Delta\rho g L^2. \tag{16}$$

Note that the left hand side of Eq. (16) is described in a manner similar to that in Eq. (10), despite being rewritten

by using Eq. (8). This introduces the Boussinesq approximation, which takes the density difference, $\Delta\rho$, to be negligible except in terms directly proportional to the density difference such as the right hand side of Eq. (16).

An additional constraint is required to solve Eq. (16) because it includes $\Delta\rho$, in contrast to Eq. (10). That leads to discussion of the conservation of volume and mass fluxes. The fluid discharged from the orifice is mixed with the ambient fluid due to vigorous turbulence. This increases the volume and mass fluxes passing through a horizontal cross-section as the fluid moves away from the orifice. Accordingly, the volume flux can be described as

$$\frac{\mathrm{d}V}{\mathrm{d}z} = V_e, \tag{17}$$

where V_e is the volume flux entrained into the turbulent region from the calm surroundings per unit height. Since the entrained mass is represented by the product of the volume of the entrained fluid and its density, the mass flux is given by

$$\frac{\mathrm{d}Q}{\mathrm{d}z} = \alpha V_e. \tag{18}$$

Combining Eqs. (17) and (18) yields

$$\frac{\mathrm{d}}{\mathrm{d}z}(\alpha V - Q) = V\frac{\mathrm{d}\alpha}{\mathrm{d}z}. \tag{19}$$

Although the right hand side of Eq. (19) can be eliminated for the flows in a uniform environment, I leave it for following arguments. Equations (6) and (7) can be used to transform Eq. (19) to

$$\frac{\mathrm{d}}{\mathrm{d}z}\left(\pi\frac{\lambda^2}{1+\lambda^2}\Delta\rho L^2 w\right) = \pi L^2 w\frac{\mathrm{d}\alpha}{\mathrm{d}z}. \tag{20}$$

Equation (20) indicates that if the ambient fluid is uniform, the buoyancy flux defined by

$$B = \pi\frac{\lambda^2}{1+\lambda^2}\frac{\Delta\rho}{\alpha}gL^2 w \tag{21}$$

remains constant. Combining Eqs. (16) and (21) yields

$$\frac{\mathrm{d}}{\mathrm{d}z}\left(\frac{\pi}{2}\alpha L^2 w^2\right) = \frac{(1+\lambda^2)\alpha B}{w}. \tag{22}$$

The buoyancy flux is independent of the momentum, volume and mass fluxes because the buoyancy flux is constant in a uniform environment whereas the other three fluxes vary with height as shown in Eqs. (16)–(18). Thus, we can envisage an ideal turbulent plume that is generated by a buoyancy flux of a finite amount given at a virtual point source without the momentum, volume, and mass fluxes at the point. This ideal turbulent plume should be described by the buoyancy flux given at the source alone. This indicates that the turbulent plume has no characteristic parameters with the dimensions of length, as is the case with turbulent jets. It therefore follows as before that the flow becomes self-similar and the radius must be directly proportional to the height:

$$L = k_p z, \tag{23}$$

where k_p is a proportionality constant for a turbulent plume.

Combining Eqs. (22) and (23) yields the upward velocity:

$$w = \left[\frac{3(1+\lambda^2)B}{2\pi k_p^2}z^{-1} + Cz^{-3}\right]^{1/3}, \tag{24}$$

where C is an integration constant and becomes zero with a boundary condition assuming a momentum flux of zero at the origin. The density difference between the inside and outside of the plume can be written as

$$\Delta\rho = \frac{\alpha}{\lambda^2 g}\left[\frac{2(1+\lambda^2)^2 B^2}{3\pi^2 k_p^4}\right]^{1/3} z^{-5/3}. \tag{25}$$

The above solution is equivalent to that obtained in Morton et al. (1956), although the entrainment assumption is not used here.

It should be noted that the equation for the volume flux, Eq. (17), holds only when the volume of entrained fluid does not change upon mixing. Actual fluids change their volume when the thermodynamic conditions in the turbulent plume differ from those of the surroundings. The air mixed into a volcanic eruption column, in particular, should significantly expand when the mixed air is heated in the eruption column. This is the key topic discussed in this paper.

Entrainment assumption

It is worth noting here a simple fact first pointed out by Batchelor (1954): The entrainment assumption is not an independent assumption but a fundamental consequence of the similarity arguments for a turbulent plume in a uniform environment. The entrainment assumption states that the increasing rate of the vertical volume flux in a turbulent plume is directly proportional to the product of the length of the circumference and upward velocity at the height, i.e.,

$$\frac{\mathrm{d}V}{\mathrm{d}z} = 2\pi\varepsilon_p L w, \tag{26}$$

where ε_p is a constant called the entrainment coefficient. This assumption was widely used in previous studies on

volcanic eruption columns since its usefulness was demonstrated by Morton et al. (1956).

In contrast, the analytical solution of turbulent plumes in the preceding subsection was derived on the basis of similarity arguments. The volume flux of Eq. (6) can be given as follows by using the similarity solution in Eqs. (23) and (24):

$$V = \pi \left[\frac{3(1+\lambda^2)k_p^4 B}{2\pi} \right]^{1/3} z^{5/3}. \tag{27}$$

The z-derivative of Eq. (27) yields an equation in which the entrainment coefficient is represented by

$$\varepsilon_p = \frac{5}{6} k_p. \tag{28}$$

In fact, if two relations of $L \propto z$ and $w \propto z^a$ (a is an arbitrary constant except -2) are simultaneously satisfied, we always obtain

$$\frac{\mathrm{d}}{\mathrm{d}z}(L^2 w) \propto L w. \tag{29}$$

This demonstrates that turbulent jets as well as turbulent plumes satisfy the relation stated in the entrainment assumption. Here, the entrainment coefficient for a turbulent jet, ε_j, is given by

$$\varepsilon_j = \frac{1}{2} k_j. \tag{30}$$

Forced plumes in a uniform environment

Forced plumes are affected by both the buoyancy flux and momentum flux given at the source. A forced plume is driven near the source predominantly by the momentum flux given at the source. Buoyancy forces increase the momentum flux at all heights as the fluid in a forced plume moves away from the source and, thus, the effect of the momentum flux given at the source becomes negligible. Accordingly, the flow asymptotically approaches a pure turbulent plume with increasing height.

The transition height from a turbulent jet to a turbulent plume can be estimated by simple dimensional analysis. Morton (1959) demonstrated that combining the constant buoyancy flux, B, and the momentum flux given at the source, M_o, yields only one parameter that has the dimension of length, given by

$$h_j = \frac{M_o^{3/4}}{\alpha^{3/4} B^{1/2}}. \tag{31}$$

Papanicolaou and List (1988)performed laboratory experiments and reported that flows behave like pure jets for $z/h_j<1$ and pure plumes for $z/h_j>5$. There is a smooth transition from jets to plumes for $1<z/h_j<5$.

I now consider the vertical variation of the momentum flux in a forced plume by using the analytical solution for turbulent plumes in Eq. (24). Note that simple similarity arguments cannot be directly applied here in the strict sense because forced plumes have a characteristic length scale, h_j. Nevertheless, laboratory experiments indicate that the spreading rate of the plume radius is nearly equal to that of the jet radius. For example, Papanicolaou and List (1988) indicated that k_j=0.109 and k_p=0.105. Accordingly, I tentatively apply the similarity solution for a pure plume to a forced plume, and then Eq. (24) gives the upward velocity of a forced plume as

$$w = \left[\frac{3(1+\lambda^2)B}{2\pi k_p^2} z^{-1} + \left(\frac{2M_o}{\pi k_p^2 \alpha} \right)^{3/2} z^{-3} \right]^{1/3}. \tag{32}$$

As expected, Eq. (32) corresponds to Eq. (12) if the buoyancy flux B is absent and k_p=k_j.

The vertical variations of the radius and upward velocity are given, and thus, the vertical variation of the momentum flux can be easily derived as

$$M = M_o \left[1 + \frac{3}{4} \left(\frac{\pi}{2} \right)^{1/2} (1+\lambda^2) k_p \left(\frac{z}{h_j} \right)^2 \right]^{2/3}. \tag{33}$$

Equation (33) suggests that the momentum flux varies by $1.1<M/M_o<3.2$ in the smooth transition range of $1<z/h_j<5$ if k_p=0.10 and λ=1.0. The middle value of the range almost exactly coincides with M/M_o=2.0, at which the momentum flux generated by buoyancy forces becomes equivalent to that given at the origin. Although this is a direct consequence of the fact that a forced plume is a composite of a pure jet and pure plume, it is noteworthy in the context of a study of volcanic eruption columns. The transition height from the gas-thrust region to the convective region of a volcanic eruption column is often prescribed by conditions different from those based on the momentum flux ratio. I will discuss this in detail in a subsequent section.

An alternative formulation of a forced plume was proposed by Morton (1959), in which a numerical integration was performed on the assumption that the entrainment coefficient is constant throughout the height. Combining Eqs. (28) and (30) under this assumption yields

$$\frac{k_p}{k_j} = \frac{3}{5}. \tag{34}$$

This suggests that the spreading rate of the radius in the plume-like region far from the origin is 40% smaller than that in the jet-like region near the origin. List and Imberger (1973) followed this treatment and derived the expression for the vertical variation of momentum flux similar to Eq. (33).

Another formulation separates a forced plume into jet-like and plume-like regions to perform numerical integration, as demonstrated in Woods (1988). Woods (1988) used the value k_j=0.125 for the jet-like region and ε_p=0.09 for the plume-like region, corresponding to k_p=0.108. Thus, the ratio of the radius spreading was

$$\frac{k_p}{k_j} = 0.864. \tag{35}$$

This indicates that Woods (1988) took an intermediate path between that based on constant radius spreading and that based on the constant entrainment coefficient.

Turbulent plumes in a stratified environment

Plumes in a linearly density-stratified environment

I next consider a flow discharged into an environment in which the fluid density varies linearly with height. Such a flow always includes some features of a plume because density stratification affects the flow via buoyancy forces. Thus, I briefly describe here only a plume not affected by the momentum flux at the origin.

The main difference between a turbulent plume in a stratified environment and one in a uniform environment is that the former has a maximum height to which it can rise. The density in the plume increases as the fluid rises because it mixes with the ambient heavier fluid. The ambient fluid is, on the other hand, less dense at higher levels when the fluid is stably stratified. Thus, the plume in a stratified fluid should reach a height at which the density in the plume is equal to that in the surroundings. This height is often referred to as the neutral buoyancy height. The direction of buoyancy forces change to downward above this height, and thus the fluid tends to stagnate near this height and spread horizontally.

Simple similarity arguments cannot be applied to the plumes in a stratified environment in the strict sense because the neutral buoyancy height characterizes the length scale of the flow. Nevertheless, Morton et al. (1956) reported that a one-dimensional model using the entrainment assumption exhibited good agreement with experimental results, even though the entrainment assumption is an alternative expression of self-similarity. This implies that density stratification has little effect on the dynamics of turbulent plumes below the neutral buoyancy height.

The above argument can be confirmed by comparing the Morton et al. (1956) model with the numerical model using the assumption that the radius is directly proportional to the height. The Morton et al. (1956) model consists of Eqs. (16), (20), and (26), i.e.,

$$\begin{cases} \dfrac{\mathrm{d}}{\mathrm{d}z}\left(\dfrac{\pi}{2}\alpha_o L^2 w^2\right) = \pi\lambda^2\Delta\rho g L^2, \\ \dfrac{\mathrm{d}}{\mathrm{d}z}\left(\pi\dfrac{\lambda^2}{1+\lambda^2}\Delta\rho L^2 w\right) = \pi L^2 w\dfrac{d\alpha}{dz}, \\ \dfrac{\mathrm{d}}{\mathrm{d}z}(\pi L^2 w) = 2\pi\varepsilon_p L w, \end{cases} \tag{36}$$

where α_o denotes the density of the ambient fluid at z=0. The relation in which the radius is directly proportional to height can be used instead of the entrainment assumption. The equation set is then given by

$$\begin{cases} \dfrac{\mathrm{d}}{\mathrm{d}z}\left(\dfrac{\pi}{2}\alpha_o L^2 w^2\right) = \pi\lambda^2\Delta\rho g L^2, \\ \dfrac{\mathrm{d}}{\mathrm{d}z}\left(\pi\dfrac{\lambda^2}{1+\lambda^2}\Delta\rho L^2 w\right) = \pi L^2 w\dfrac{d\alpha}{dz}, \\ L = k_p z. \end{cases} \tag{37}$$

Figure 1 depicts the numerical integrations of the two equation sets above. The physical variables are normalized as with Morton et al. (1956) by

$$\begin{cases} z &= 2^{-3/4}\pi^{-1/4}(1+\lambda^2)^{-1/8}\varepsilon_p^{-1/2}B_o^{1/4}N^{-3/4}x, \\ L &= 2^{1/4}\pi^{-1/4}(1+\lambda^2)^{-1/8}\varepsilon_p^{1/2}B_o^{1/4}N^{-3/4}R, \\ w &= 2^{1/4}\pi^{-1/4}(1+\lambda^2)^{3/8}\varepsilon_p^{-1/2}B_o^{1/4}N^{1/4}U, \\ g\dfrac{\Delta\rho}{\alpha_o} &= 2^{-3/4}\pi^{-1/4}\lambda^{-2}(1+\lambda^2)^{7/8}\varepsilon_p^{-1/2}B_o^{1/4}N^{5/4}\Delta, \end{cases} \tag{38}$$

where B_o is the buoyancy flux given at the origin and N is the parameter that characterizes the stratification of the environment, defined by

$$N^2 = -\frac{g}{\alpha_o}\frac{\mathrm{d}\alpha}{\mathrm{d}z}. \tag{39}$$

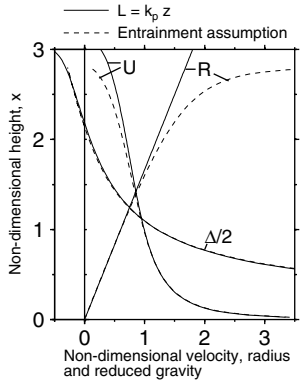

Fig. 1 The variation of the non-dimensional upward velocity (U), radius (R), and reduced gravity ($\Delta/2$) with height calculated for a turbulent plume in a uniformly and stably stratified fluid. The solid lines are calculated by Eq. (37), which assumes the radius to be directly proportional to the height. The dashed lines signify the calculation with the equation set derived by Morton et al. (1956) shown in Eq. (36). Note that two lines of $\Delta/2$ are too close to be distinguished

This parameter is often referred to as the Brunt-Väisälä frequency.

The radius obtained from the Morton et al. (1956) model is almost the same as that from Eq. (37) below the neutral buoyancy height, x=2.1, as shown in Fig. 1. This indicates that the entrainment assumption can be applied because the density stratification has little effect on the spreading rate of the plume radius. The upward velocity and reduced gravity as well as the radius obtained from the two equation sets are consequently very similar.

Note that the similarity solution to the turbulent plume in a uniform environment can also be regarded as a fairly good approximation. I can clarify that by estimating the neutral buoyancy height using Eq. (25). The density at the centerline in the turbulent plume, β, is given by

$$\beta = \alpha_o - \frac{\alpha_o}{\lambda^2 g}\left[\frac{2(1+\lambda^2)^2 B_o^2}{3\pi^2 k_p^4}\right]^{1/3} z^{-5/3}. \tag{40}$$

The density of the ambient stratified fluid can be written as

$$\alpha = \alpha_o + \frac{\mathrm{d}\alpha}{\mathrm{d}z} z. \tag{41}$$

Since the density inside and outside of the plume becomes equal at the neutral buoyancy height, i.e., α=β, the height can be estimated from

$$z = 2^{1/8} 3^{-1/8} \pi^{-1/4} \lambda^{-3/4} (1+\lambda^2)^{1/4} k_p^{-1/2} B_o^{1/4} N^{-3/4}. \tag{42}$$

Letting λ=1.0 and k_p=1.2 ε_p gives a value of 1.9 in non-dimensional form as the neutral buoyancy height, while the numerical integration of Morton et al. (1956) yields 2.1.

Plumes in an isentropic atmosphere

I next discuss turbulent plumes rising in an isentropic atmosphere to examine the effect of a decrease in atmospheric pressure with height. Air is compressible, and thus the atmospheric pressure decreases with increasing height, even if the atmosphere is in neutral equilibrium. This compressibility makes the fluid in the turbulent plumes expand as they rise. This requires substantial modification in the model for turbulent plumes because the models in the previous sections are based on the assumption that the discharged fluid and its surroundings do not change their volume.

Since the pressure in a plume, P, is assumed to be equal to the pressure of the ambient atmosphere, it is given by the hydrostatic equation:

$$\frac{\mathrm{d}P}{\mathrm{d}z} = -\alpha g. \tag{43}$$

Combining Eq. (43) with a simple thermodynamic relation, $C_a\, dT$=dP/α, which is always satisfied in an adiabatic process, yields the temperature of an isentropic atmosphere at a given height z:

$$T^* = T_o - \frac{g}{C_a} z, \tag{44}$$

where C_a is the air specific heat at a constant pressure, and T_o is the air temperature at ground level. The density of the atmosphere decreases with increasing height as the pressure and temperature decrease with height.

The conservation of fundamental physical variables, i.e., momentum, mass, and volume fluxes, are re-examined to take the volume change due to the air compressibility into account. Equations (16) and (18) can be used as they are written because the momentum and mass fluxes are not affected by the air compressibility. However, the volume flux equation in Eq. (17) must be modified to add the volume change due to compressibility, δV, to the right hand side. Thus, the equation set for a turbulent plume in an isentropic atmosphere can be written by

$$\begin{cases} \dfrac{\mathrm{d}}{\mathrm{d}z}\left(\dfrac{\pi}{2}\alpha L^2 w^2\right) & = \pi\lambda^2 \Delta\rho g L^2, \\ \dfrac{\mathrm{d}}{\mathrm{d}z}\left[\pi\left(\alpha - \dfrac{\lambda^2}{1+\lambda^2}\Delta\rho\right) L^2 w\right] & = \alpha V_e, \\ \dfrac{\mathrm{d}}{\mathrm{d}z}(\pi L^2 w) & = V_e + \delta V. \end{cases} \tag{45}$$

Note that the density difference $\Delta\rho$ is neglected on the left hand side of the momentum flux equation in the same manner as in Eq. (16).

Morton et al. (1956) suggested that the one-dimensional model for incompressible turbulent plumes can be applied to turbulent plumes in the atmosphere by replacing the *in-situ* density with potential density. The potential density, α^*, is the density that a fluid element would have if moved adiabatically to a constant reference pressure; here, the pressure at ground level, P_o. The potential density of an ideal gas can be written as

$$\alpha^* = \left(\frac{P}{P_o}\right)^{-1/\gamma} \alpha, \tag{46}$$

where γ is the ratio of specific heats for air. The potential density, α^*, is now constant at all heights and equal to the air density at the ground level from the definition of an isentropic atmosphere.

The replacement of the in-situ density by potential density in the one-dimensional model implies that Eq. (45) is transformed to

$$\begin{cases} \dfrac{\mathrm{d}}{\mathrm{d}z}\left(\dfrac{\pi}{2}\alpha^* L^{*2} w^2\right) & = \pi\lambda^2 \Delta\rho^* g L^{*2}, \\ \dfrac{\mathrm{d}}{\mathrm{d}z}\left[\pi\left(\alpha^* - \dfrac{\lambda^2}{1+\lambda^2}\Delta\rho^*\right) L^{*2} w\right] & = \alpha^* V_e^*, \\ \dfrac{\mathrm{d}}{\mathrm{d}z}\left(\pi L^{*2} w\right) & = V_e^*, \end{cases} \tag{47}$$

with the parameters defined by

$$L^* = \left(\frac{P}{P_o}\right)^{1/2\gamma} L, \tag{48}$$

and

$$V_e^* = \left(\frac{P}{P_o}\right)^{1/\gamma} V_e. \tag{49}$$

Here, $\Delta\rho^*$ is the potential density that corresponds to the density difference between the fluid on the centerline and the undisturbed surroundings. The ratio of specific heats of the outside the plume is assumed to be equivalent to that in the plume. The third expression in Eq. (47) includes the volume change due to compressibility (see Appendix A for details). The form of Eq. (47) is the same as the equation set from which the similarity solution for a turbulent plume in a uniform environment is derived. Accordingly, the similarity solution can be obtained in a comparable manner if the modified radius L^* is assumed to be proportional to the height, although the validity of this assumption is unclear.

The simple similarity arguments cannot be directly applied to a turbulent plume in an isentropic atmosphere because the temperature profile in the isentropic atmosphere yields a parameter with the dimensions of length, h_a, given by

$$h_a = \frac{C_a T_o}{g}. \tag{50}$$

Furthermore, Eq. (47) suggests that a decrease in the atmospheric pressure causes the expansion of the plume radius without any major departure of the vertical motion from that predicted by the similarity solution of a turbulent plume in a uniform environment. This greatly simplifies the mathematical treatment and allows us to use the model with the potential density to estimate the height to which a plume in a stratified fluid can rise, as is the case in a plume of an incompressible fluid. However, the validity of this modification is unclear, mainly because the difference in pressure between inside and outside of a plume may considerably affect the motion under the conditions considered here.

It should also be noted that L^* and V_e^* have the following relationship if the entrainment assumption in the form of Eq. (26) holds:

$$V_e^* = 2\pi \left(\frac{P}{P_o}\right)^{1/2\gamma} \varepsilon_p L^* w. \tag{51}$$

This indicates that the formulation using the entrainment assumption cannot preserve the mathematical equivalence between the turbulent plumes in a uniform environment and that discussed in this subsection. This discrepancy makes little difference when the plume height is lower than the height h_a, at which $(P/P_o)^{1/\gamma}$ is considerably less than unity.

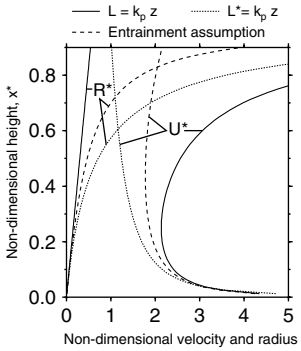

Fig. 2 The variation with height of the non-dimensional upward velocity (U^*) and radius (R^*) calculated for a turbulent plume in an isentropic atmosphere. The dotted lines are calculated by Eq. (47) with the assumption that the modified radius is proportional to the height, while the dashed lines are obtained from the entrainment assumption in Eq. (51). The solid lines signify the result with the original radius proportional to the height

Figure 2 illustrates the vertical variation of the radius and upward velocity obtained from Eq. (47) with three different conditions. Figure 2 is drawn with non-dimensional variables derived in Appendix B. The original radius L expands with increasing height following Eq. (48) if L^* is proportional to the height. The corresponding upward velocity is the same as that given by Eq. (24). If L is directly proportional to height, the upward velocity sharply increases with height above x^*=0.5, i.e., a half of the height h_a. The velocity is almost the same as that for $L^*=k_p\, z$ only below x^*=0.1. The calculation using the entrainment assumption yields intermediate results between the above two conditions as expected from Eq. (51). It is noteworthy that the calculation with the entrainment assumption also predicts that the upward velocity increases with height above x^*=0.5.

Volcanic eruption columns

I now discuss a one-dimensional model for volcanic eruption columns consisting of a hot gas-particle mixture. The effects of thermal expansion of the mixed air as well as the decrease in the atmospheric pressure are taken into consideration by using an argument comparable to that in the preceding subsection. This derives a model equivalent to the Woods (1988) model.

The solid particles suspended in an eruption column are assumed to be so fine that the particles and the ambient gas are in thermal and dynamic equilibrium, as considered in many theoretical studies on eruption columns. This implies that the temperature of the particles is the same as that of the ambient gas, and settling of the particles is negligible. The gas-particle mixture can then be treated as a homogeneous continuum, the bulk density of which can be represented by averaging the density of each component. The equation of the state of the gas-particle mixture can be described as

$$\frac{1}{\beta} = \frac{nR_gT}{P} + \frac{1-n}{\rho_s}, \tag{52}$$

where the gas component in an eruption column is assumed to behave as a perfect gas. n is the mass fraction of the gas component, R_g is the bulk gas constant for the gas component, T is the temperature in an eruption column, and ρ_s is the density of the solid particles. Alternatively, the equation of the state can be described with the volume fraction of the gas component, ϕ, as

$$\beta = \phi\rho_g + (1-\phi)\rho_s, \tag{53}$$

where ρ_g is the density of the gas component in the eruption column, i.e., ρ_g=P/R_gT.

The pressure in an eruption column is assumed to be the same as the ambient atmosphere at all heights. This assumption should be used with caution because the exit velocity at the volcanic vent may be supersonic during some volcanic eruptions. A one-dimensional model should be modified to include the decompression at the basal part of an eruption column, as discussed in Woods and Bower (1995), though this is beyond the scope of this paper. This paper also does not consider the effect of the inner dense core, which is thought to be immediately above a volcanic vent, due to insufficient mixing with the surroundings. These assumptions allow us to directly extend the similarity arguments to the model of an eruption column.

The momentum and mass fluxes in Eqs. (16) and (18) can be directly applied to the volcanic eruption columns, as is the case with plumes in the isentropic atmosphere. It is assumed here that the time-averaged profiles in the horizontal cross-section are a top-hat distribution instead of a Gaussian distribution to compare the obtained results with those in Woods (1988). Equations (16) and (18) are then modified to

$$\frac{\mathrm{d}}{\mathrm{d}z}(\pi\beta L^2w^2) = \pi\Delta\rho g L^2, \tag{54}$$

and

$$\frac{\mathrm{d}}{\mathrm{d}z}(\pi\beta L^2 w) = \alpha V_e. \tag{55}$$

Note that the Boussinesq approximation is not applied to Eq. (54) because a typical bulk density of a juvenile gas-particle mixture immediately above a volcanic vent is substantially larger than the surrounding air density.

The equation of volume flux was used in previous subsections on the assumption that the volume of the fluid in question can be specified even if the thermodynamic state is not completely determined. The equation of energy conservation should now be combined with the equation of state to consider volume change due to a change in temperature as well as pressure. Also considered here is the equation for volume flux of the gas component in an eruption column to compare the one-dimensional model for an eruption column with that described in previous subsections. The volume flux equation is actually required to complete the model because the gas mass fraction is included as an additional variable in the system of an eruption column.

The volume of gas in an eruption column changes as the temperature and pressure change with height even if the surrounding air is not entrained at all. Also, the air entrained into an eruption column changes its volume because the air is heated and expands. Accordingly, the equation for volume flux of the gas component is given by

$$\frac{\mathrm{d}}{\mathrm{d}z}(\pi\phi L^2 w) = V_e + \delta V + \delta V_e, \tag{56}$$

where δV is the volume change of the gas component in the eruption column due to the temperature and pressure change, excluding the influence of the entrained air, which can be written as

$$\delta V = -\pi\phi L^2 w \frac{T}{P}\frac{\mathrm{d}}{\mathrm{d}z}\left(\frac{P}{T}\right). \tag{57}$$

Note that the bulk gas constant does not vary with height unless the surrounding air is entrained. The volume change of the entrained air due to its thermal expansion, δV_e, is given by

$$\delta V_e = -\frac{V_e}{\alpha}\frac{\mathrm{d}\alpha}{\mathrm{d}T}(T - T_a), \tag{58}$$

where T_a is the temperature of the ambient air. Combining Eqs. (56) to (58) yields

$$\frac{\mathrm{d}}{\mathrm{d}z}(\pi\phi L^2 w) = \frac{T}{T_a}V_e - \pi\phi L^2 w\frac{\mathrm{d}}{\mathrm{d}z}\left[\ln\left(\frac{P}{T}\right)\right]. \tag{59}$$

The energy flux equation is that in Woods (1988):

$$\frac{\mathrm{d}}{\mathrm{d}z}\left[\pi\beta\left(C_pT + \frac{w^2}{2} + gz\right)L^2w\right] = \alpha(C_aT + gz)V_e, \tag{60}$$

where C_p is the bulk specific heat at constant pressure. Heat transfer without mass transfer, such as thermal diffusion and radiation, is neglected to derive Eq. (60), on the assumption that the heat transfer due to a mass transfer caused by vigorous turbulence (i.e., entrainment) is predominant over other heat transfer processes. Equation (60) can be easily transformed to the equation for enthalpy flux:

$$\frac{\mathrm{d}}{\mathrm{d}z}(\pi\beta C_pTL^2w) = \alpha\left(C_aT_a + \frac{w^2}{2}\right)V_e - \pi\alpha g L^2 w. \tag{61}$$

As a result, the equation set to be solved becomes

$$\begin{cases} \dfrac{1}{\beta} & = \dfrac{nR_gT}{P} + \dfrac{1-n}{\rho_s}, \\ \dfrac{\mathrm{d}}{\mathrm{d}z}(\pi\beta L^2 w^2) & = \pi\Delta\rho g L^2, \\ \dfrac{\mathrm{d}}{\mathrm{d}z}(\pi\beta L^2 w) & = \alpha V_e, \\ \dfrac{\mathrm{d}}{\mathrm{d}z}(\pi\phi L^2 w) & = \dfrac{T}{T_a}V_e - \pi\phi L^2 w\dfrac{\mathrm{d}}{\mathrm{d}z}\left[\ln\left(\dfrac{P}{T}\right)\right], \\ \dfrac{\mathrm{d}}{\mathrm{d}z}(\pi\beta C_p T L^2 w) & = \alpha\left(C_aT_a + \dfrac{w^2}{2}\right)V_e - \pi\alpha g L^2 w, \end{cases} \tag{62}$$

where R_g and C_p are the functions of n given by

$$R_g = R_a + (R_m - R_a)\frac{n_o(1-n)}{(1-n_o)n}, \tag{63}$$

and

$$C_p = C_a + (C_{po} - C_a)\frac{1-n}{1-n_o}. \tag{64}$$

R_a is the gas constant for air, R_m is the gas constant for the gas component at a volcanic vent, n_o is the gas mass fraction at the vent, and C_{po} is the bulk specific heat at constant pressure at the vent. The derivations of R_g and C_p are described in Appendix C with some other notes on Woods (1988). Equation (62) becomes equivalent to the equation set in Woods (1988) when combining the entrainment assumption used in Woods (1988):

$$V_e = \begin{cases} 2\pi\varepsilon_j L w\left(\dfrac{\beta}{\alpha}\right)^{1/2} & \text{if } \alpha(z') < \beta(z') \quad \text{for all } z' \le z, \\ 2\pi\varepsilon_p L w & \text{otherwise.} \end{cases} \tag{65}$$

I next transform Eq. (62) to find a form that corresponds to Eq. (47). As described in Appendix D in detail, Eq. (59) is equivalent to

$$\frac{\mathrm{d}}{\mathrm{d}z}(\pi n\beta L^2 w) = \alpha V_e. \tag{66}$$

By introducing

$$L^\dagger = \left(\frac{n\beta}{\alpha_o}\right)^{1/2} L, \tag{67}$$

and

$$V_e^\dagger = \frac{\alpha}{\alpha_o}V_e, \tag{68}$$

Eq. (66) can be rewritten as

$$\frac{\mathrm{d}}{\mathrm{d}z}(\pi L^{\dagger 2} w) = V_e^\dagger. \tag{69}$$

Similarly, Eq. (62) can be rewritten as

$$\begin{cases} \dfrac{1}{\beta} & = \dfrac{nR_gT}{P} + \dfrac{1-n}{\rho_s}, \\ \dfrac{\mathrm{d}}{\mathrm{d}z}\left(\dfrac{\pi L^{\dagger 2} w^2}{n}\right) & = \pi\dfrac{\Delta\rho}{n\beta} g L^{\dagger 2}, \\ \dfrac{\mathrm{d}}{\mathrm{d}z}\left(\dfrac{\pi L^{\dagger 2} w}{n}\right) & = V_e^\dagger, \\ \dfrac{\mathrm{d}}{\mathrm{d}z}\left(\pi L^{\dagger 2} w\right) & = V_e^\dagger, \\ \dfrac{\mathrm{d}}{\mathrm{d}z}\left(\dfrac{\pi C_p T L^{\dagger 2} w}{n}\right) & = \left(C_aT_a + \dfrac{w^2}{2}\right)V_e^\dagger \\ & \quad -\pi\dfrac{\alpha}{n\beta} g L^{\dagger 2} w. \end{cases} \tag{70}$$

It is obvious that the modified radius $L^\dagger$ is the straightforward extension of L^* even though the equation set in Eq. (70) does not use the potential density. Equation (67) can be rewritten in a form similar to Eq. (48) as

$$L^\dagger = \left(\frac{\phi R_a T^*}{R_g T}\right)^{1/2}\left(\frac{P}{P_o}\right)^{1/2\gamma} L. \tag{71}$$

It should be noted that T^* is different from T_a, in contrast to a plume in an isentropic atmosphere described in the preceding section, because I am now considering the motion in a more realistic atmosphere.

The model is completed by combining Eq. (70) with the entrainment assumption or an alternative relationship between the radius and height. I numerically investigate the sensitivity of the dynamics of volcanic eruption columns to the formulation of the model with the entrainment assumption and its alternatives in the next section.

Numerical investigation

Integration conditions

Numerical integrations under the following three different conditions were performed to examine the sensitivity of the physical properties in an eruption column to the radius variation with height. The first condition combines Eq. (62) with the entrainment assumption described in Eq. (65). Obviously, this yields the same results as Woods (1988). The result of the Woods (1988) model is shown here only for reference as it was extensively discussed in the original paper. The second condition is the numerical integration of Eq. (70) with the assumption that the modified radius $L\dagger$ can be described as

$$\frac{\mathrm{d}L^\dagger}{\mathrm{d}z} = \begin{cases} \left(\dfrac{\beta}{\alpha}\right)^{1/2} k_j & \text{if } \alpha(z') < \beta(z') \quad \text{for all } z' \le z, \\ k_p & \text{otherwise.} \end{cases} \tag{72}$$

This is referred to as *an inflation model*. The inflation model can be regarded as an extreme case in which a decrease in the atmospheric pressure and a thermal expansion of the gas component increases the plume radius as much as possible without affecting the vertical motion. The third condition is the numerical integration of Eq. (62), in which the radius L is given by

$$\frac{dL}{dz} = \begin{cases} \left(\frac{\beta}{\alpha}\right)^{1/2} k_j & \text{if } \alpha(z') < \beta(z') \quad \text{for all } z' \le z, \\ k_p & \text{otherwise,} \end{cases} \tag{73}$$

which is referred to as *a cone model*. The decrease in the atmospheric pressure and the thermal expansion of the gas component in the cone model do not affect the plume radius at all. The cone model can be regarded as another extreme case, opposite to the inflation model.

The numerical integrations were performed under the atmospheric conditions described in Appendix E. I used a fourth-order Runge-Kutta scheme with a step size of 5 m in the calculations.

Note that the inflation model and cone model give unrealistic results above the neutral buoyancy height because the radius is prescribed as a function of height, regardless of the value of the upward velocity in an eruption column. This inconsistency occurs because the fundamental assumption that lateral motion is negligible compared with vertical motion becomes invalid near the neutral buoyancy height. In fact, this violation of the assumption may even limit the validity of the Woods (1988) model, as Glaze and Baloga (2002) noted. Thus, the focus in this paper is on properties below the neutral buoyancy height.

In addition, the cone model may make the volume of entrained air a negative amount. This is clearly dynamically inconsistent, because a minus value of entrained air indicates that some fluids in the turbulent region abruptly become at rest as they rise. To avoid this discrepancy, I replace the momentum flux equation in Eq. (62) with the condition that $V^{\dagger}=0$ if the cone model makes the entrained volume a minus value. This treatment allows the upward velocity in an eruption column to increase with height. This may occur in actual eruption columns because the pressure in the column would become greater than the ambient pressure when the column cannot sufficiently expand in the lateral direction. The calculation under this condition is indicated by a dotted line in the figures.

Effect of the vent radius

The first calculation was performed with the following vent conditions at ground level: a temperature of 1000 K, exit velocity of 300 m s^{-1}, gas mass fraction of 0.03 and vent radii of 20, 100, and 300 m. These conditions yield a bulk density at the vent of 7.25 kg m^{-3}. The results of the inflation model and the Woods (1988) model are presented in Fig. 3. The fundamental features obtained from the two

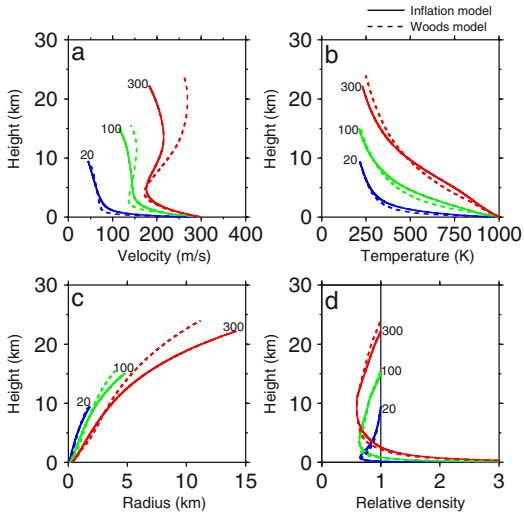

Fig. 3 The variation of properties in a volcanic eruption column with the height calculated by the inflation model and Woods (1988) model for w_o=300 m s^{-1}, T_o=1000 K, n_o=0.03, and L_o=20, 100, 300 m. (**a**) Velocity. (**b**) Temperature. (**c**) Radius. (**d**) Relative density

models are similar. For example, the larger the vent radius, the higher the eruption column reaches. The column properties predicted by the inflation model for a vent radius of L_o=20 m in particular are almost the same as that of Woods (1988). The differences between the two models become significant as the vent radius increases.

The inflation model predicts wider column radii than the Woods (1988) model at the upper part. The column radius of the inflation model was only 0.10 km larger than that of the Woods (1988) model at z=9 km for L_o=20 m. The differences in the column radii between two models were 0.20 km at z=10 km and 3.17 km at z=20 km for L_o=300 m. The difference of column radii between two models became significant about 10 km above the vent. This implies that the radius expansion above 10 km in the inflation model causes greater entrainment of the surrounding air than the Woods (1988) model.

The qualitative nature of the relative density variation of the inflation model is similar to that of Woods (1988). This makes the column height of the inflation model almost the same as that of Woods (1988). The neutral buoyancy heights obtained from the inflation model were 9.48, 15.1, and 22.2 km for L_o=20 m, 100 m, and 300 m, while the Woods (1988) model yielded 9.25, 15.5, and 24.0 km, respectively.

The velocity of the inflation model was lower than that of the Woods (1988) model at the upper part of the eruption columns while the inflation model yielded the gentler slope of velocity decrease with height at the lower part. It is notable that the inflation model indicates a monotonic decrease of column velocity with height for L_o=20 m and 100 m. This implies that deceleration due to momentum transfer to the entrained air tends to exceed acceleration due to upward buoyancy forces in the inflation model, and thus the velocity decreases with height throughout the eruption column over a wider parameter range than that of the Woods (1988) model.

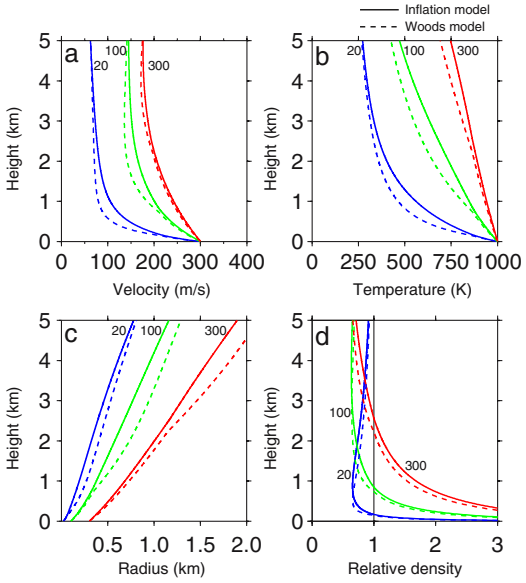

Fig. 4 The property variation with height in the lower part of the column calculated by the inflation model and Woods (1988) model for w_o=300 m s^{-1}, T_o=1000 K, n_o=0.03, and L_o=20, 100, 300 m. (**a**) Velocity. (**b**) Temperature. (**c**) Radius. (**d**) Relative density

Figure 4 presents the properties of the lower 5 km of the column obtained from the same calculation as that shown in Fig. 3. The result of the inflation model is very similar to that of the Woods (1988) model at the region in which the bulk density in the column is greater than the ambient density. This implies that the formulation of the entrainment assumption in Woods (1988) for $\alpha<\beta$ includes an effect similar to the modification of the radius described in Eq. (67). The inflation model makes the radius smaller for the region presented in Fig. 4 than that of the Woods (1988) model. As a result, the velocity and temperature remains greater than that obtained from the Woods (1988) model. The relative density is also greater than that of Woods (1988) model for the region in which the relative density decreases with height.

Figure 5 illustrates the results of the cone model in a manner similar to Fig. 3. The radius is directly proportional to the height, as prescribed for the model condition. This condition significantly inhibits ambient air from being entrained into the eruption column. As a result, the vertical variation of column properties differs considerably from that of Woods (1988), in particular for L_o=300 m. The calculation for L_o=300 m indicates that the columns continue rising above 30 km, whereas the bulk density remains greater than the ambient density. The upward velocity continues increasing with height above 5 km and becomes 645 m s^{-1} at 30 km. The temperature remains higher than 750 K at a height of 30 km. In contrast to the result of the inflation model, the calculation for L_o=20 m also differs significantly from that of the Woods (1988) model. This is clearly evident at the lower part of the eruption column in Fig. 6. The radius of the cone model is 233 m less than that of the Woods (1988) model for L_o=20 m at 5 km, while

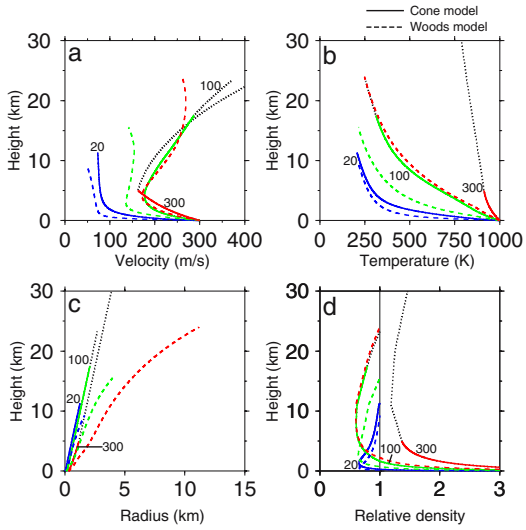

Fig. 5 The variation of properties in a volcanic eruption column with height calculated by the cone model and Woods (1988) model for w_o=300 m s^{-1}, T_o=1000 K, n_o=0.03, and L_o=20, 100, 300 m. (**a**) Velocity. (**b**) Temperature. (**c**) Radius. (**d**) Relative density

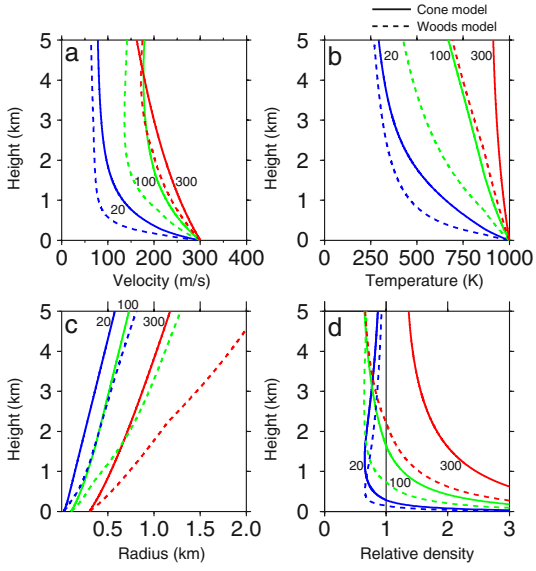

Fig. 6 The property variation with height in the lower part of the column calculated by the cone model and Woods (1988) model for w_o=300 m s^{-1}, T_o=1000 K, n_o=0.03, and L_o=20, 100, 300 m. (**a**) Velocity. (**b**) Temperature. (**c**) Radius. (**d**) Relative density

the inflation model yields a radius only 29 m less than that of the Woods (1988).

Figure 7 presents the neutral buoyancy height as a function of the vent radius. The conditions at the vent were the same as those shown in 3–6 except for the vent radius. The cone model yields the greatest neutral buoyancy height of the three models. The heights of the cone model results are 24% higher for L_o=10 m and 76% higher for L_o=150 m than those of the Woods (1988) model. The inflation model yields smaller heights than the Woods (1988) model, although the difference is only 16% at most.

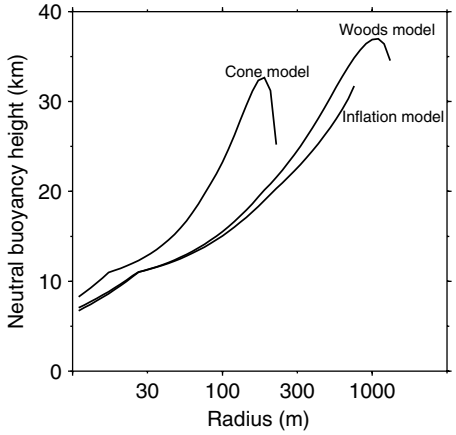

Fig. 7 The neutral buoyancy height as a function of the vent radius calculated with w_o=300 m s^{-1}, T_o=1000 K, n_o=0.03

The bulk density may remain greater than the ambient density in a calculation with a large vent radius, and thus we cannot define the neutral buoyancy height. That explains why none of the three lines reach the right end of the graph. The line for the result of the Woods (1988) model is closest to the right end in Fig. 7. This implies that the Woods (1988) model predicts that column collapse does not occur for a relatively larger vent radius, if following Woods (1988) in which a similar figure is used to determine the conditions for column collapse. However, an eruption column may continue rising while the bulk density remains greater than the ambient density as illustrated in Fig. 5. Thus, Fig. 7 should be interpreted with caution. I will discuss this further in the discussion section.

Effect of gas mass fractions at a vent

Next is an examination of how the column properties vary with the gas mass fractions at a vent. The calculation is performed with a temperature of 1000 K, exit velocity of 300 m s^{-1}, vent radius of 100 m, and gas mass fractions at the vent of 0.01, 0.03, and 0.05. These conditions make the bulk density at the vent 21.43, 7.25, and 4.36 kg m^{-3}. The results of the inflation model are presented in Fig. 8, and those of the cone model in Fig. 9. The results of the Woods (1988) model are also provided in the figures for comparison. The fundamental tendency of the results obtained from the Woods (1988) model is relatively similar to those of the inflation model. The vertical variation of the relative density of the Woods (1988) model is, in particular, almost the same as that of the inflation model. As a result, the two models yield similar column heights.

As the gas mass fraction decreases, the results of each model deviate from those of the Woods (1988) model in a similar manner to the results of each model obtained with increasing radius. These results are expected because the terms including βL^2 play important roles in the governing equation set described in Eq. (62). The mass, momentum, and enthalpy fluxes are all directly proportional to βL^2. Besides, β can be regarded as inversely proportional to n

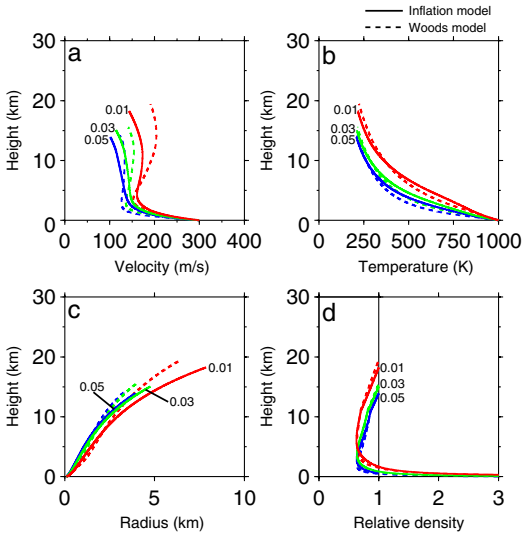

Fig. 8 The variation of properties in a volcanic eruption column with the height calculated by the inflation model and Woods (1988) model for w_o=300 m s^{-1}, T_o=1000 K, L_o=100 m, and n_o=0.01, 0.03, 0.05. (**a**) Velocity. (**b**) Temperature. (**c**) Radius. (**d**) Relative density

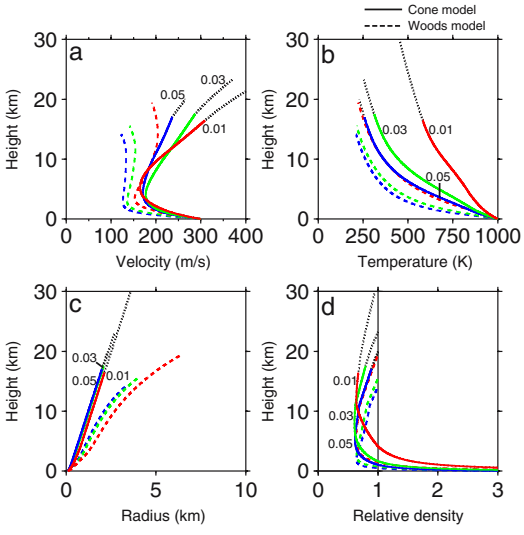

Fig. 9 The variation of properties in a volcanic eruption column with the height calculated by the cone model and Woods (1988) model for w_o=300 m s^{-1}, T_o=1000 K, L_o=100 m, and n_o=0.01, 0.03, 0.05. (**a**) Velocity. (**b**) Temperature. (**c**) Radius. (**d**) Relative density

if n is large enough (see Eq. (52)). A detailed parametric study shows that the calculations of each model with different values of L_o and n_o yields similar results except for the bulk density immediately above the volcanic vent as long as $L_o{}^2/n_o$ remains constant. For example, the result of the calculation with L_o=100 m and n_o=0.01 displayed in Fig. 8 is similar to that with L_o=173 m and n_o=0.03.

Mass, momentum, and buoyancy fluxes

Figure 10 illustrates the variations of the mass, momentum, and buoyancy fluxes with height, which were obtained from

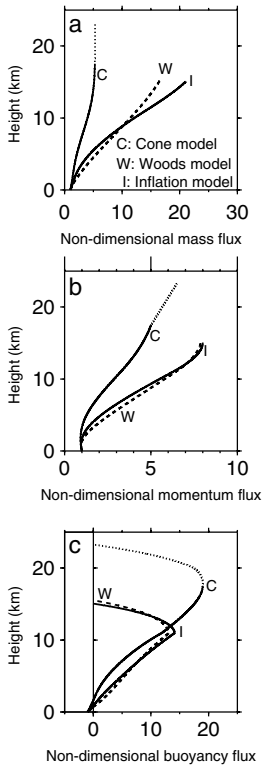

Fig. 10 The variation of fundamental fluxes in a volcanic eruption column with height. (**a**) Mass flux. (**b**) Momentum flux. (**c**) Buoyancy flux

a calculation with a vent temperature of 1000 K, exit velocity of 300 m s^{-1}, gas mass fraction of 0.03, and vent radius of 100 m. Each flux is normalized by the value at the vent such as Q/Q_o, M/M_o, and $B/|B_o|$ in Fig. 10. Each of the three fluxes of the Woods (1988) model exhibits a variation similar to that of the inflation model.

The mass flux increases with increasing height as a result of the entrainment of the ambient air. The mass flux of the cone model is less than a half of that of the Woods (1988) model above 3 km and only 30% at a height of 15 km, while the differences between the inflation model and the Woods (1988) model are less than 30% at all heights. The increasing rate of the mass flux of the inflation model is the greatest of the three models above 3 km. This implies that the pressure decrease with height suppresses the air entrainment not only in the cone model but also in the Woods (1988) model.

The momentum flux also increases with increasing height in most of the column. However, the momentum flux slightly decreases with height at the basal part of the column, at which the bulk density in the column is greater than the ambient density. This occurs because the momentum flux increases due to buoyancy forces. The cone model has a wider basal part than others at which part the eruption column retains the bulk density greater than the ambient density, and thus its momentum flux remains small. The momentum flux of the cone model is less than that at the ground surface below 3.25 km and twice as much as that at 7.60 km. The Woods (1988) model yields the greatest momentum flux among the three models in most of the column. The momentum flux above 1.30 km is greater than that at the ground surface and twice as much as that at 3.93 km.

The profiles of the buoyancy flux in Fig. 10 exhibit the most essential difference between volcanic eruption columns and turbulent plumes of an incompressible fluid. The buoyancy flux in an eruption column significantly increases with height at the lower part, while that in incompressible plumes cannot increases with height in a stably stratified fluid (see Eq. (20)). This occurs because the thermal expansion of entrained air and the decrease in the atmospheric pressure with height considerably change the volume of the gas component in an eruption column.

Examining the above three fluxes enables us to clarify the distinguishing characteristics of the dynamics of volcanic eruption columns. The result indicates that the generation of momentum flux due to buoyancy is suppressed at the basal part of the eruption columns because volcanic eruption columns sustain many solid particles that minimize the buoyancy forces at the lower part. This makes the height at which the momentum flux generated by buoyancy becomes as large as that given at the vent, i.e., the height where $M=2M_o$ in an eruption column, much higher than h_j, which represents the corresponding height for a typical forced plume of a constant buoyancy flux (see Eq. (33)). The height of $M=2M_o$ is also much greater than the height where the bulk density in the column exceeds the ambient density. This implies that a volcanic eruption column can be regarded as a turbulent jet over wider ranges of parameters than previously thought, if the implications of the laboratory experiments by Papanicolaou and List (1988) can be applied.

The transition condition from a gas-thrust region to a convective region has been treated ambiguously in previous studies. Woods (1988) considered that the transition occurred at the height at which the density in an eruption column becomes less than the ambient density. Sparks and Wilson (1976) defined the limit of the gas-thrust region as the height at which the minimum upward velocity occurs. While each of the above two heights provides meaningful information, the abrupt transition at each height brings unrealistic discontinuity to the vertical profiles of physical variables, as discussed in Glaze (1999). The smooth transition near a height of $M=2M_o$ is consistent with the discussion in this paper and, thus, this height may be useful as an alternative index.

Discussion

The dynamics of volcanic eruption columns have been discussed in previous studies primarily using the entrainment assumption, which was originally introduced for an incompressible turbulent plume. However, the underlying physics stated in the entrainment assumption are derived from similarity arguments based on the fact that the buoyancy flux of an incompressible turbulent plume remains constant in a uniform environment. In contrast, the

buoyancy flux of an eruption column varies significantly with height, as illustrated in Fig. 10. Accordingly, great caution is required when applying the entrainment assumption to a one-dimensional model of a volcanic eruption column.

Furthermore, volcanic eruption columns generated in the real atmosphere include some length scales by which the motion of the eruption columns may depart from self-similar motion. This difference can be verified in the equation sets for an incompressible plume and an eruption column. The combination of the equation of state and enthalpy flux used in Eqs. (62) and (70) is considerably more complicated than the volume flux equation in Eq. (36). This implies that the system of an eruption column may not have a simple relation in which the volume of mixed air at a given height is exactly proportional to the product of the upward velocity and radius at that height.

Nevertheless, one-dimensional models based on the entrainment assumption have been widely employed to examine the dynamics of eruption columns. This is primarily because the model yields the relationship between the eruption column height and heat flux, which agrees well with the observation of actual volcanic eruptions. Briggs (1969) used the observation data of large oil fires to successfully demonstrate the usefulness of the Morton et al. (1956) model for estimating plume heights in the actual atmosphere from the heat flux. Settle (1978) and Wilson et al. (1978) accepted this idea and applied it to volcanic eruption columns to obtain results in reasonable agreement with the observation. Furthermore, Sparks (1986) discussed the influence of air compressibility with an approach similar to that for plumes in an isentropic atmosphere in this paper.

The relationship between the column height and heat flux derived from the Morton et al. (1956) model can be regarded as a result of a dimensional analysis for predominant variables. An alternative model based on similarity arguments predicts a comparable column height as described in Fig. 1 and Eq. (42). This suggests that the relationship may be more robust than the entrainment assumption. Thus, the relationship does not necessarily verify the entrainment assumption. Since other observation data, such as the velocity and temperature profiles in a volcanic eruption column, are sparse, there is little information regarding whether an actual eruption column obeys the entrainment assumption.

This paper examines the difference between the direct extension of similarity arguments and the Woods (1988) model, which is based on the entrainment assumption. The Woods (1988) model yields a result almost the same as that of the inflation model at the lower part of the column, where the bulk density in the column is greater than the ambient air. The discrepancy between the two models becomes significant as the column height becomes sufficiently high for the decrease in atmospheric pressure with height to affect the expansion rate of the column. This result is interpreted in the following discussions.

The analogy with the similarity solutions for simple plumes and jets leads us to expect that the entrainment rate in Eq. (65) has a simple relation with the spreading rate of the modified radius. If the entrainment assumption holds in the same way as Woods (1988), the modified expression of the entrained volume $V_e^{\dagger}$ at the higher part of the column where $\beta < \alpha$ can be written with the modified radius $L^{\dagger}$ as

$$V_e^{\dagger} = 2\pi \left(\frac{\alpha}{\beta}\right)^{1/2} \left(\frac{\alpha}{n\alpha_o}\right)^{1/2} \varepsilon_p L^{\dagger} w. \tag{74}$$

Equation (74) has a form similar to Eq. (51), which is easily identified by recalling the definition of the potential density in Eq. (46). Equation (74) indicates that the entrainment rate for an eruption column described by a modified radius varies with the density ratio between inside and outside of the column at a given height, the ratio of the air density at that height to that of the ground surface, and the mass fraction of the gas component in the column if the entrainment assumption is satisfied.

The fact that inflation model yields a result similar to that of the Woods (1988) model at the gas-thrust region implies that the Woods (1988) model corresponds to the formulation in which the density difference between the inside and outside of the eruption column does not affect the expansion rate of the column radius. Thus, the vertical gradient of the modified radius at the convective region written as

$$\frac{\mathrm{d}L^{\dagger}}{\mathrm{d}z} = \left(\frac{\alpha}{n\alpha_o}\right)^{1/2} k_p \tag{75}$$

may yield a result more similar to that of Woods (1988)than that of the inflation model. The calculation using Eq. (75) is called *the imitation model*. The lower part is the same as that of the inflation model. This calculation is depicted in Fig. 11. As expected, the result of this model is in fairly good agreement with that of the Woods (1988) model.

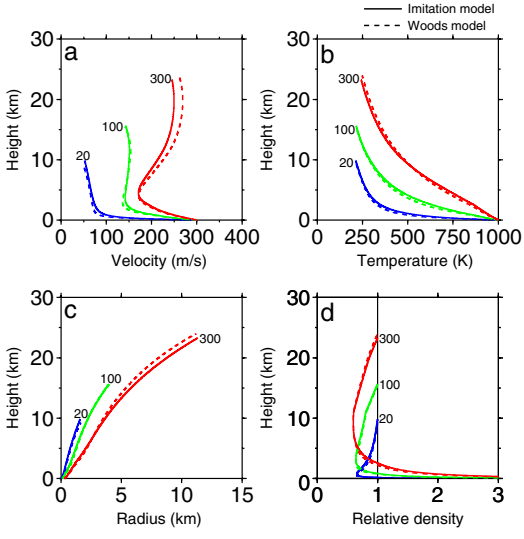

Fig. 11 The variation of properties in a volcanic eruption column with the height calculated by the imitation model and Woods (1988) model for w_o=300 m s^{-1}, T_o=1000 K, n_o=0.03, and L_o=20, 100, 300 m. (**a**) Velocity. (**b**) Temperature. (**c**) Radius. (**d**) Relative density

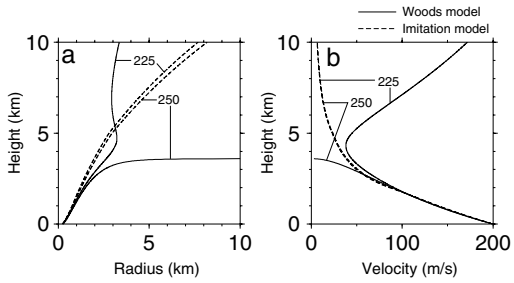

Fig. 12 The variation of properties in a volcanic eruption column with the height calculated by the imitation model and Woods (1988) model for w_o=200 m s^{-1}, T_o=1000 K, n_o=0.01, and L_o=225, 250 m. (**a**) Radius. (**b**) Velocity. Note that two lines of the imitation model are too close to be distinguished in (b)

The coincidence between the imitation model and the Woods (1988) model reveals the underlying mathematical structure of the Woods (1988) model. The density stratification in the atmosphere causes the difference between the results of the inflation model and Woods (1988) model. The temperature at the region high in the atmosphere up to 30 km is at most 25% lower than the temperature at the ground surface, while the pressure is about one-fourth at 10 km and one-hundredth at 30 km less than the pressure at the ground surface. Thus, the decrease in the atmospheric pressure can be regarded as the major cause of the difference in the results of the inflation model and Woods (1988) model. Further observations are required to determine which model is more realistic.

It should be noted that the Woods (1988) model and imitation model yield significantly different conditions for column collapse, although the two models provides similar results for stable eruption columns. Figure 12 depicts the calculation using the Woods (1988) and imitation models with a vent temperature of 1000 K, exit velocity of 200 m s^{-1}, gas mass fraction of 0.01, and vent radii of 225 m and 250 m. The calculation with the imitation model yields results of L_o=225 m and 250 m which are similar. The radii increase with height with almost a constant rate. The upward velocities decrease with height throughout heights illustrated in Fig. 12. In contrast, the calculation for L_o=250 m with the Woods (1988) model reveals a rapid increase of the radius at a height above 3 km. The upward velocity decreased with height and the column ceased to rise at 3.6 km. The calculation using L_o=225 m yielded the upward velocity that increased with height above 4.3 km. The radius decreased at heights between 4.7 and 6.9 km.

The above differences exist because the radius in the Woods (1988) model may vary with the upward velocity following the entrainment assumption, while the radius in the imitation model is prescribed independently of the velocity. This difference in the formulation yields significant differences in the results particularly when the upward velocity approaches zero with the bulk density in the eruption column greater than the ambient density. The high density makes the buoyancy forces negative and thus reduces the momentum flux. This causes an abrupt reduction of the upward velocity, while the mass flux continues increasing with height due to air entrainment. As a result, the radius of the Woods (1988) model sharply increases with height to compensate for the velocity reduction to continue increasing the mass flux if the density remains greater than the ambient air density.

This indicates that column collapse conditions derived from the Woods (1988) model are governed by the algebraic structure of the entrainment assumption, although the assumption is not thoroughly verified for such specific conditions. In fact, the horizontal motion is no longer negligible at a height at which the radius of the eruption column sharply increases with height. This violates a fundamental assumption of one-dimensional models; thus, it may be beyond the ability of one-dimensional models to prescribe conditions for column collapse.

The principal uncertainty inherent in one-dimensional eruption column models is directly related to the shape of an eruption column if the boundary conditions at a volcanic vent can be specified by the constraint on the flow in a volcanic conduit. If the governing equations of eruption columns in Eq. (62) are combined with actual observation data of the vertical variation of column radius, the model provides more realistic features of eruption columns. Fortunately, fine solid particles suspended in an eruption column allow us to easily determine the outer shape of the eruption column. This suggests that appropriate observations of eruption columns can reduce the uncertainty of the model. Existing photographs and video recordings may provide meaningful information regarding the dependences of the entrainment coefficient on gas compressibility.

Thorough physical measurements during actual volcanic eruptions are important to clarify the relationship between column shape and the vertical variations of other physical variables. The analysis performed by Sparks and Wilson (1982), for example, should be extended to stratosphere-penetrating eruption columns. An accumulation of observational data is crucial particularly for examining the column collapse condition.

Conclusions

This paper extends the similarity arguments for turbulent jets and plumes to volcanic eruption columns to explicitly describe the underlying physics stated in the entrainment assumption. This enables examination of the effect of compressibility of the gas component in an eruption column. The buoyancy flux in an eruption column varies significantly with height due to gas compressibility. This causes considerable uncertainties in the similarity solution. The uncertainties cause at most 70% of the errors in estimation of column height. Although the new model and the Woods (1988) model yield similar results for stably sustained eruption columns, there are marked discrepancies in the prediction of column collapse. The uncertainty of the model is directly related to the variation of column radius with height, and thus it is essential to capture the column shape during actual eruptions to obtain reliable information from one-dimensional models.

Appropriate diagnostic measurements of eruption column shapes are required, particularly during the eruptions under conditions close to those causing column collapses.

Acknowledgements The author would like to thank Lionel Wilson, Greg Valentine, and James White for their helpful comments and suggestions on an earlier version of this paper. The author would also like to acknowledge useful discussions with Yoshiaki Ida and Takehiro Koyaguchi on the ideas presented in this paper.

Appendix A: Derivation of modified radius

The modified radius L^* introduced in Eq. (48) can be obtained by considering the steady mass flux of an ideal gas flowing adiabatically without entrainment of the surroundings. Let us consider a vertical flow in a disk with a radius of L and a density of α, as in the main body of this paper. The mass flux in the disk remains constant if no ambient air is entrained into the disk, and then it can be written as

$$\frac{\mathrm{d}}{\mathrm{d}z}(\pi\alpha L^2 w) = 0. \tag{A1}$$

The potential density described by Eq. (46) remains constant if the air in the disk is moved adiabatically. Combining Eq. (A1) with Eq. (46) yields

$$\frac{\mathrm{d}}{\mathrm{d}z}\left[\pi L^2 w \left(\frac{P}{P_o}\right)^{1/\gamma}\right] = 0. \tag{A2}$$

Equation (A2) can be transformed to

$$\frac{\mathrm{d}}{\mathrm{d}z}(\pi L^2 w) = -\frac{\pi L^2 w}{\gamma P}\frac{\mathrm{d}P}{\mathrm{d}z}, \tag{A3}$$

which represents the volume flux variation with height. This indicates that the right hand side of Eq. (A3) corresponds to δV in Eq. (45). Since Eq. (A2) is obviously equivalent to Eq. (A3), the volume flux equation can be described with the modified radius L^* as

$$\frac{\mathrm{d}}{\mathrm{d}z}(\pi L^{*2} w) = 0. \tag{A4}$$

Note that we have a simple relation

$$\alpha L^2 = \alpha^* L^{*2}, \tag{A5}$$

and thus Eq. (A1) can be described in a similar form by using L^* instead of L:

$$\frac{\mathrm{d}}{\mathrm{d}z}(\pi\alpha^* L^{*2} w) = 0. \tag{A6}$$

The modified radius for volcanic eruption columns defined by Eq. (67) can be derived in a similar way.

Appendix B: Derivation of non-dimensional variables

The model for a turbulent plume in an isentropic atmosphere is transformed to a non-dimensional form to derive the parameters used in Fig. 2. If the entrainment assumption is satisfied, Eq. (47) can be deduced as

$$\begin{cases} \dfrac{\mathrm{d}}{\mathrm{d}z}(L^{*2}w^2) = \dfrac{2(1+\lambda^2)B^*}{\pi w}, \\ \dfrac{\mathrm{d}}{\mathrm{d}z}(L^{*2}w) = 2(\dfrac{P}{P_o})^{1/2\gamma}\varepsilon_p L^* w, \end{cases} \tag{B1}$$

where B^* is constant, defined by

$$B^* = \pi\frac{\lambda^2}{1+\lambda^2}\frac{\Delta\rho^*}{\alpha^*}gL^{*2}w. \tag{B2}$$

Equation (B1) can be rewritten as follows by introducing new variables defined by $X{=}L^* w$ and $Y{=}L^{*2}w$:

$$\begin{cases} \dfrac{\mathrm{d}X^4}{\mathrm{d}z} = \dfrac{4(1+\lambda^2)B^*}{\pi}Y, \\ \dfrac{\mathrm{d}Y}{\mathrm{d}z} = 2(\dfrac{P}{P_o})^{1/2\gamma}\varepsilon_p X. \end{cases} \tag{B3}$$

When I choose the following variables,

$$\begin{cases} z = h_a x^*, \\ X = 2\pi^{-1/3}(1+\lambda^2)^{1/3}\varepsilon_p^{1/3}h_a^{2/3}B^{*1/3}\xi, \\ Y = 4\pi^{-1/3}(1+\lambda^2)^{1/3}\varepsilon_p^{4/3}h_a^{5/3}B^{*1/3}\psi, \end{cases} \tag{B4}$$

I can transform Eq. (B3) to the simplest non-dimensional form:

$$\begin{cases} \dfrac{\mathrm{d}\xi^4}{\mathrm{d}x^*} = \psi, \\ \dfrac{\mathrm{d}\psi}{\mathrm{d}x^*} = (1-x^*)^{5/4}\xi. \end{cases} \tag{B5}$$

Here, I use the approximation

$$C_a = \frac{7}{2}R_a. \tag{B6}$$

The above transformation yields the non-dimensional forms of the radius and upward velocity used in Fig. 2 as

$$\begin{cases} L^* = 2\varepsilon_p h_a(1-x^*)^{5/4}R^*, \\ w = \pi^{-1/3}(1+\lambda^2)^{1/3}\varepsilon_p^{-2/3}h_a^{-1/3}B^{*1/3}U^*. \end{cases} \tag{B7}$$

Appendix C: Note on Woods (1988)

Woods (1988) derived a number of useful relations among physical variables to discuss the dynamics of volcanic eruption columns. I will interpret some of the relations here because the physical background of the mathematical treatment in Woods (1988) is not always clear.

I first derive Eq. (63), which corresponds to Eq. (5) in Woods (1988), by considering the total volume of the gas component in an eruption column at a given height. The gas component in an eruption column consists of the volcanic gas ejected from a vent and the air entrained from the surroundings. If the gas component in an eruption column behaves as an ideal gas, then the volume of the gas component can be written as

$$\frac{m_g R_g T}{P} = \frac{m_m R_m T}{P} + (m_g - m_m)\frac{R_a T}{P}, \tag{C1}$$

where m_g is the total mass of the gas component in an eruption column at the height, and m_m is the mass of the volcanic gas at a vent. Equation (C1) yields

$$R_g = R_a + \frac{m_m}{m_g}(R_m - R_a). \tag{C2}$$

The total mass of the gas component m_g has the following relations with the total mass of solid particles m_s:

$$n = \frac{m_g}{m_g + m_s}, \tag{C3}$$

$$1 - n = \frac{m_s}{m_g + m_s}. \tag{C4}$$

Similarly, the mass of the volcanic gas m_m has the following relations:

$$n_o = \frac{m_m}{m_m + m_s}, \tag{C5}$$

$$1 - n_o = \frac{m_s}{m_m + m_s}. \tag{C6}$$

Combining Eqs. (C3) to (C6) yields

$$\frac{m_m}{m_g} = \frac{n_o(1-n)}{(1-n_o)n}. \tag{C7}$$

Equation (63) can be obtained from Eqs. (C2) and (C7).

The bulk specific heat at a constant pressure of the whole substance in an eruption column can be derived in a similar way. The enthalpy variation with temperature in an eruption column is written as

$$(m_g + m_s)C_p dT = (m_g - m_m)C_a dT + (m_m + m_s)C_{po} dT. \tag{C8}$$

Thus,

$$C_p = C_a + \frac{m_m + m_s}{m_g + m_s}(C_{po} - C_a). \tag{C9}$$

Combining Eqs. (C4), (C6), and (C9) yields Eq. (64).

Next, I consider the expression for the bulk density in Woods (1988):

$$\beta = \frac{\beta_o L_o^2}{L^2}\left[\frac{w_o}{w} + n_o \frac{R_m}{R_a}\left(\frac{\phi L^2 P T_o}{\phi_o L_o^2 P_o T} - \frac{w_o}{w}\right)\right], \tag{C10}$$

where each variable with a subscript o represents a value evaluated at a volcanic vent. This expression can be obtained from the relation for the volume flux of the gas component at a given height, $\phi L^2 w$, which can be regarded as the sum of the volume flux of the gas component from the volcanic vent and that of the total air entrained throughout heights lower than the given height, i.e.,

$$\frac{n\beta L^2 w}{\rho_g} = \frac{n_o \beta_o L_o^2 w_o}{\rho_m} + \frac{\beta L^2 w - \beta_o L_o^2 w_o}{\rho_b}, \tag{C11}$$

where the relation of $n\beta = \phi\rho_g$ is used. Here, ρ_m represents the density of the gas at the vent and moved to the height, i.e., $P/R_m T$. Similarly ρ_b represents the density of the mixed air in the eruption columns at the height, $P/R_a T$. Equation (C11) can be rewritten as

$$\left(\frac{nR_g}{R_a} - 1\right)\beta L^2 w = \left(\frac{n_o R_m}{R_a} - 1\right)\beta_o L_o^2 w_o, \tag{C12}$$

which is easily transformed to Eq. (C10).

I introduce here the equation of the mass flux of solid particles. The mass of solid particles does not change with height because the air entrained into the eruption columns from the surroundings contains no solid particles. Thus, the equation of solid mass flux can be expressed as

$$\frac{\mathrm{d}}{\mathrm{d}z}[\pi(1-n)\beta L^2 w] = 0. \tag{C13}$$

From Eq. (C13), I can easily deduce

$$(1-n)\beta L^2 w = (1-n_o)\beta_o L_o^2 w_o, \tag{C14}$$

which is equivalent to Eq. (4) in Woods (1988). Note that Eq. (A10) in Woods (1988) is also equivalent to Eq. (C13).

In addition, using a relation of $(1-n)\beta = (1-\phi)\rho_s$ with constant ρ_s can transform Eq. (C13) to

$$\frac{\mathrm{d}}{\mathrm{d}z}(\pi L^2 w) = \frac{\mathrm{d}}{\mathrm{d}z}(\pi\phi L^2 w). \tag{C15}$$

Equation (C15) indicates that the total change of volume flux in an eruption column is equal to that of the gas component. Combining Eqs. (55), (59), and (C15) to eliminate

V_e yields

$$\frac{\mathrm{d}}{\mathrm{d}z}(\pi\beta L^2 w) = \rho_g \frac{R_g}{R_a}\left\{\frac{\mathrm{d}}{\mathrm{d}z}(\pi L^2 w) + \pi\phi L^2 w \frac{\mathrm{d}}{\mathrm{d}z}\left[\ln\left(\frac{P}{T}\right)\right]\right\} \tag{C16}$$

which is easily transformed to Eq. (A6) in Woods (1988).

Appendix D: Alternative derivation of the volume flux equation for volcanic eruption columns

The equation of volume conservation for the gas component in a volcanic eruption column presented in Eq. (59) can be derived more easily although I carefully considered the thermodynamic conditions in the main body of this paper by following Woods (1988).

Similar to the mass conservation equation for the whole substance in an eruption column described by Eq. (55), the mass conservation equation for the gas component can be given by

$$\frac{\mathrm{d}}{\mathrm{d}z}(\pi n\beta L^2 w) = \alpha V_e. \tag{D1}$$

Note that Eq. (D1) can be derived from Eqs. (55) and (C13). The relation $n\beta = \phi\rho_g$ allows transformation of Eq. (D1) to

$$\frac{\mathrm{d}}{\mathrm{d}z}(\pi\phi L^2 w) = \frac{\alpha}{\rho_g} V_e - \frac{\pi\phi L^2 w}{\rho_g}\frac{\mathrm{d}\rho_g}{\mathrm{d}z}. \tag{D2}$$

We can easily determine that Eq. (D2) is equivalent to Eq. (59) by combining two simple relations:

$$\frac{1}{\rho_g}\frac{\mathrm{d}\rho_g}{\mathrm{d}z} = \frac{\mathrm{d}}{\mathrm{d}z}\left[\ln\left(\frac{P}{T}\right)\right] - \frac{1}{R_g}\frac{\mathrm{d}R_g}{\mathrm{d}z}, \tag{D3}$$

and

$$\frac{\mathrm{d}R_g}{\mathrm{d}z} = (R_a - R_g)\frac{\alpha V_e}{\pi n\beta L^2 w}. \tag{D4}$$

Appendix E: The ambient atmospheric conditions

A numerical investigation of volcanic eruption columns was performed with the same atmospheric conditions as those in Woods (1988). The atmospheric conditions are explicitly shown here because there are some errors in the description of the conditions in Woods (1988).

The temperature profile is given by

$$T_a = \begin{cases} T_o + \Gamma_1 z & \text{for } z \le H_1, \\ T_1 & \text{for } H_1 < z \le H_2, \\ T_1 + \Gamma_2 (z - H_2) & \text{for } H_2 < z, \end{cases} \tag{E1}$$

where H_1 is the height of the tropopause (11 km) and H_2 is that of the stratopause (20 km). Γ_1 and Γ_2 are the temperature lapse rate in the troposphere and stratosphere. T_1 is the temperature at H_1, corresponding to $T_o + \Gamma_1 H_1$. Combining Eq. (E1) with the hydrostatic equation in Eq. (43) yields the pressure profile as

$$P = \begin{cases} P_o \left(\frac{T_a}{T_o}\right)^{-\frac{g}{R_a\Gamma_1}} & \text{for } z \le H_1, \\ P_1 \exp\left[-\frac{g(z - H_1)}{R_a T_1}\right] & \text{for } H_1 < z \le H_2, \\ P_2 \left(\frac{T_a}{T_1}\right)^{-\frac{g}{R_a\Gamma_2}} & \text{for } H_2 < z, \end{cases} \tag{E2}$$

where P_1 and P_2 are the pressures at H_1 and H_2.

References

Batchelor GK (1954) Heat convection and buoyancy effects in fluids. Quart J R Met Soc 80:339–358

Briggs GA (1969) Plume Rise. US Atomic Energy Commission, Oak, Ridge, pp 1–81

Carey S, Sigurdsson H (1989) The intensity of plinian eruptions. Bull Volcanol 51:28–40

Dobran F (2001) Volcanic processes: mechanisms in material transport. Kluwer Academic/Plenum Publishers, New York, pp1–590

Fischer HB, List EJ, Koh RCY, Imberger J, Brooks NH (1979) Mixing in inland and coastal waters. Academic Press, New York, pp 1–483

Glaze LS (1999) Transport of SO_2 by explosive volcanism on Venus. J Geophys Res 104E8:18899–18906

Glaze LS, Baloga SM (1996) Sensitivity of buoyant plume height to ambient atmospheric conditions: Implications for volcanic eruption columns. J Geophys Res 101D1:1529–1540

Glaze LS, Baloga SM (2002) Volcanic plume heights on Mars: Limits of validity for convective models. J Geophys Res 107E10:5086, doi:10.1029/2001JE001830

Glaze LS, Baloga SM, Wilson L (1997) Transport of atmospheric water vapor by volcanic eruption columns. J Geophys Res 102D5:6099–6108

Ishimine Y (2005) Numerical study of pyroclastic surges. J Volcanol Geotherm Res 139:33–57, doi: 10.1016/j.jvolgeores.2004.06.017

Landau LD, Lifshitz EM (1987) Fluid mechanics. 2nd edn. Pergamon Press, Oxford, pp1–532

List EJ (1982) Turbulent jets and plumes. Ann Rev Fluid Mech 14:189–212

List EJ, Imberger J (1973) Turbulent entrainment in buoyant jets and plumes. Proc ASCE J Hydraul Div 99:1461–1474

Morton BR (1959) Forced plumes. J Fluid Mech 5:151–163

Morton BR, Taylor GI, Turner JS (1956) Turbulent gravitational convection from maintained and instantaneous sources. Proc R Soc London A 234:1–23

Neri A, Dobran F (1994) Influence of eruption parameters on the thermofluid dynamics of collapsing volcanic columns. J Geophys Res 99B6:11833–11857

Oberhuber JM, Herzog M, Graf HF, Schwanke K (1998) Volcanic plume simulation on large scales. J Volcanol Geotherm Res 87:29–53

Papanicolaou PN, List EJ (1988) Investigations of round vertical turbulent buoyant jets. J Fluid Mech 195:341–391

Prandtl L (1952) Essentials of fluid dynamics: with applications to hydraulics, aeronautics, meteorology and other subjects. Blackie, London, pp 1–452

Rouse H, Yih CS, Humphreys HW (1952) Gravitational convection from a boundary source. Tellus 4:201–210

Settle M (1978) Volcanic eruption clouds and the thermal power output of explosive eruptions. J Volcanol Geotherm Res 3:309–324

Sparks RSJ (1986) The dimensions and dynamics of volcanic eruption columns. Bull Volcanol 48:3–15

Sparks RSJ, Wilson L (1976) A model for the formation of ignimbrite by gravitational column collapse. J Geol Soc London 132:441–451

Sparks RSJ, Wilson L (1982) Explosive volcanic eruptions – V. Observations of plume dynamics during the 1979 Soufriere eruption, St Vincent. Geophys J R Astr Soc 69:551–570

Sparks RSJ, Bursik MI, Carey SN, Gilbert JS, Glaze LS, Sigurdsson H, Woods AW (1997) Volcanic plumes. John Wiley & Sons Ltd, Chichester, pp1–574

Turner JS (1986) Turbulent entrainment: the development of the entrainment assumption, and its application to geophysical flows. J Fluid Mech 173:431–471

Valentine GA, Wohletz KH (1989) Numerical models of plinian eruption columns and pyroclastic flows. J Geophys Res 94B2:1867–1887

Walker GPL (1981) Plinian eruptions and their products. Bull Volcanol 44:221–240

Wilson L (1976) Explosive volcanic eruptions - III. Plinian eruption columns. Geophy J R Astr Soc 45:543–556

Wilson L, Sparks RSJ, Huang TC, Watkins ND (1978) The control of volcanic column heights by eruption energetics and dynamics. J Geophys Res 83B4:1829–1836

Woods AW (1988) The fluid dynamics and thermodynamics of eruption columns. Bull Volcanol 50:169–193

Woods AW (1993) The dynamics of explosive volcanic eruptions. Rev Geophys 33:495–530

Woods AW, Bursik MI (1991) Particle fallout, thermal disequilibrium and volcanic plumes. Bull Volcanol 53:559–570

Woods AW, Bower SM (1995) The decompression of volcanic jets in a crater during explosive volcanic eruptions. Earth Planet Sci Lett 131:189–205